


2006

# Utilization of sulfur dioxide in organic acids recovery and sulfur trioxide conversion with iron oxide as catalyst

Yonghui Shi  
*Iowa State University*

Follow this and additional works at: <https://lib.dr.iastate.edu/rtd>

 Part of the [Civil Engineering Commons](#), and the [Environmental Engineering Commons](#)

## Recommended Citation

Shi, Yonghui, "Utilization of sulfur dioxide in organic acids recovery and sulfur trioxide conversion with iron oxide as catalyst " (2006). *Retrospective Theses and Dissertations*. 1486.  
<https://lib.dr.iastate.edu/rtd/1486>

This Dissertation is brought to you for free and open access by the Iowa State University Capstones, Theses and Dissertations at Iowa State University Digital Repository. It has been accepted for inclusion in Retrospective Theses and Dissertations by an authorized administrator of Iowa State University Digital Repository. For more information, please contact [digirep@iastate.edu](mailto:digirep@iastate.edu).

Utilization of sulfur dioxide in organic acids recovery and sulfur trioxide conversion with  
iron oxide as catalyst

by

Yonghui Shi

A dissertation submitted to the graduate faculty  
in partial fulfillment of the requirements for the degree of  
DOCTOR OF PHILOSOPHY

Major: Civil Engineering (Environmental Engineering)

Program of Study Committee:  
J. Hans van Leeuwen (Co-major Professor)  
Robert C. Brown (Co-major Professor)  
Shihwu Sung (Co-major Professor)  
Thomas D. Wheelock  
Roy Gu

Iowa State University

Ames, Iowa

2006

UMI Number: 3223019

UMI<sup>®</sup>

---

UMI Microform 3223019

Copyright 2006 by ProQuest Information and Learning Company.  
All rights reserved. This microform edition is protected against  
unauthorized copying under Title 17, United States Code.

---

ProQuest Information and Learning Company  
300 North Zeeb Road  
P.O. Box 1346  
Ann Arbor, MI 48106-1346

Graduate College  
Iowa State University

NOTE:  
Electronic theses  
will not contain  
the signed thesis  
approval page  
here.

## TABLE OF CONTENT

<b>ABSTRACT.....</b>	<b>v</b>
<b>CHAPTER 1. GENERAL INTRODUCTION .....</b>	<b>1</b>
1. Introduction.....	1
2. Dissertation Organization .....	5
3. Literature Review.....	5
3.1. Recovery of Acetic Acid and Lactic Acid with SO <sub>2</sub> .....	5
3.2. Oxidation of SO <sub>2</sub> with Microscale and Nanoscale Fe <sub>2</sub> O <sub>3</sub> as Catalysts.....	9
References.....	11
<b>CHAPTER 2. THE RECOVERY OF ACETIC ACID WITH SULFUR DIOXIDE .....</b>	<b>18</b>
Abstract.....	18
1. Introduction.....	19
2. Materials and Methods.....	21
2.1. Materials .....	21
2.2. Apparatus and Operational Procedures.....	21
2.3. Analysis of Acetic Acid with HPLC.....	22
3. Results and Discussion .....	23
4. Conclusions.....	26
Acknowledgement .....	26
References.....	27
<b>CHAPTER 3. THE EXTRACTION OF LACTIC ACID WITH SULFUR DIOXIDE .</b>	<b>31</b>
Abstract.....	31
1. Introduction.....	32
2. Materials and Methods.....	34
2.1. Reagents.....	34
2.2. Apparatus .....	34
2.3. Operational Procedures.....	35
2.4. Analysis of Lactic Acid with HPLC.....	35
3. Results and Discussion .....	36
4. Conclusions.....	38
Acknowledgement .....	39
References.....	39
<b>CHAPTER 4. CATALYTIC OXIDATION OF SULFUR DIOXIDE WITH MICROSCALE AND NANOSCALE IRON OXIDES AS CATALYSTS .....</b>	<b>43</b>
Abstract.....	43
1. Introduction.....	44
2. Experimental Section.....	46
2.1. Materials .....	46
2.2. Surface Area Measurement.....	47
2.3. Structure Characterization with Transmission Electron Microscopy .....	47

2.4. Determination of Total Iron .....	47
2.5. Determination of $Fe^{2+}$ and $Fe^{3+}$ .....	48
3. Results and Discussion .....	52
3.1. Structure of Microscale and Nanoscale $Fe_2O_3$ .....	52
3.2. Baseline .....	52
3.3. Effects of Temperatures .....	53
3.4. Reaction Orders for $SO_2$ and Oxygen .....	53
3.5. Reaction Constant $k$ and Apparent Activation Energy $E_a$ .....	58
3.6. The Reaction Mechanism of $SO_2$ Catalytic Oxidation .....	60
References .....	61
<b>CHAPTER 5. GENERAL CONCLUSIONS .....</b>	<b>78</b>
<b>APPENDIX .....</b>	<b>81</b>
<b>ACKNOWLEDGEMENT .....</b>	<b>86</b>

**ABSTRACT**

Sulfur dioxide (SO<sub>2</sub>) is a primary air pollutant and its emission is strictly restricted by pertinent regulations. Methodology is to use SO<sub>2</sub> as a raw material to produce valuable chemicals while purifying the flue gas. Two approaches that use SO<sub>2</sub> in the flue gas were put forward and examined. In the first approach, SO<sub>2</sub> was used to recover acetic acid and lactic acid from the biological process. The second approach converted SO<sub>2</sub> to SO<sub>3</sub> through oxidation with iron oxide (Fe<sub>2</sub>O<sub>3</sub>) as catalyst. The experimental results of acetic and lactic acid recovery showed that both the reaction time and breakthrough time decreased with the increase of reaction temperature and SO<sub>2</sub> flow rate. Analysis of the produced acetic and lactic acids demonstrated that the complete conversion of organic calcium salts to corresponding organic acids was not affected by the reaction conditions. The findings of this study indicated that recovering acetic acid and lactic acid with SO<sub>2</sub> is both economical and environmentally beneficial. The oxidation of SO<sub>2</sub> was greatly enhanced by either microscale or nanoscale Fe<sub>2</sub>O<sub>3</sub> according to the experiment results. Nanoscale Fe<sub>2</sub>O<sub>3</sub> performed much better than its microscale counterpart in catalyzing the SO<sub>2</sub> oxidation. The conversion of SO<sub>2</sub> was temperature dependent for both types of Fe<sub>2</sub>O<sub>3</sub>. The reaction orders with respect to the reactants sulfur dioxide and oxygen were determined when using microscale and nanoscale iron oxides as catalysts. Empirical Arrhenius expressions of the catalytic oxidation of sulfur dioxide oxidation were derived based on rate constants obtained at different temperatures.

## CHAPTER 1. GENERAL INTRODUCTION

### 1. Introduction

One of the most abundant elements that compose the earth, sulfur is prevalent in most fossil fuels, such as coals and crude oils. The power plants and many other industries that burn fossil fuel, as well as vehicles using high sulfur diesel, release more than 156 million tons of sulfur dioxide ( $\text{SO}_2$ ) into the atmosphere globally each year [1], causing serious environmental pollution.  $\text{SO}_2$  is the main cause of acid rain and its emission is strictly restricted by many national or international regulations and treaties. Acid rain is rather harmful to the natural environment, leading to the corrosion of buildings, acidification of water bodies and the deterioration of local and even global ecosystems. Once inhaled,  $\text{SO}_2$  is detrimental to the respiratory tract of human beings. Those individuals, including children, elders and patients with heart or lung diseases, are especially sensitive to  $\text{SO}_2$  [2,3].

$\text{SO}_2$  is classified as one of the six primary air pollutants that must be prevented from releasing to the environment because of its hazardous effect on the environment and human health. Most power plants resort to new technologies to reduce their  $\text{SO}_2$  emission to meet the stringent emission standard. These technologies include both new combustion processes that remove  $\text{SO}_2$  or prevent it from forming during coal combustion, and new pollution control facilities that clean  $\text{SO}_2$  from flue gases before they are released to the atmosphere. The commonly used  $\text{SO}_2$  reduction methods include fluidized bed combustion (FBC), flue gas desulfurization (FGD), corona discharge and integrated gasification combined cycle (IGCC) system.



FBC system burns coal in a fluidized bed in the presence of the sorbents, such as limestone or dolomite, to facilitate the capture of  $\text{SO}_2$ . The injected limestone undergoes decomposition in the combustion chamber of the FBC due to rapid heat accumulation from incineration to produce calcium oxide and carbon dioxide [4,5].  $\text{SO}_2$  originates from the oxidation of sulfur contained in the coal. It reacts with the calcium oxide to form calcium sulfite or calcium sulfate. The produced calcium sulfite and calcium sulfate can be readily disposed along with the combustion ash

FGD is the most popular  $\text{SO}_2$  reduction method, which allows for a  $\text{SO}_2$  emission reduction up to 99% [6]. The FGD technologies can be classified in four groups: wet-scrubber, spray-dry scrubber, dry-scrubber and combined  $\text{SO}_2/\text{NO}_x$  removal-process technologies. Among those technologies, the wet scrubber technology is most frequently used and takes up more than 80% of market share. The wet scrubber FGD technology is based on the adsorption of  $\text{SO}_2$  with limestone slurry. The flue gas passes through the scrubber where limestone slurry is sprayed and  $\text{SO}_2$  is removed. The slurry is then collected in a tank where the sulfite oxidation, limestone dissolution and gypsum crystallization take place. The produced gypsum has to be dewatered and can be used for manufacturing of gypsum board or land filling [7].

The energetic electron induced plasma process is one of the most effective methods for simultaneous removal of  $\text{SO}_2$  and  $\text{NO}_x$  from the flue gas. The commonly used non-thermal plasma methods include pulsed corona discharge, barrier discharge and DC discharge. Among all of these methods, pulsed corona discharge process has been given more attention recently. Pilot scale tests showed that more than 95 % of  $\text{SO}_2$  in the flue gas was successfully removed by using this method [8-10]. If water vapor exists in the flue gas, the high relative

humidity will create a suitable condition for the existence of the radical reactions, which is believed to dominate the removal process of  $\text{SO}_2$  [11]. Although pulsed corona discharge is effective in  $\text{SO}_2$  removal, the high energy requirement and non-uniformity on the produced oxidizing radicals are two major problems that need to be solved [12].

In the IGCC system, coal gasification takes place in the presence of a controlled shortage of air or oxygen, thus maintaining a reducing condition. The sulfur present in the coal is essentially reduced to hydrogen sulfide ( $\text{H}_2\text{S}$ ). Considering the fact that  $\text{H}_2\text{S}$  is more readily removed than  $\text{SO}_2$ , treatment of IGCC flue gas will be relatively less complicated. Solid regenerable sorbents of mixed-metal oxides that efficiently remove  $\text{H}_2\text{S}$  and carbonyl sulfide have been developed. A test with ZnO-doped manganese oxide sorbent as regenerable sorbent also showed its high efficiency in removing  $\text{H}_2\text{S}$  [13]. Using a copper based absorbent, a  $\text{H}_2\text{S}$  concentration of less than 1 ppmv was obtained in the temperature range of 350~450 °C [14].

Although the aforementioned methods can effectively remove  $\text{SO}_2$ , they normally produce large amounts of by-products. These by-products are either of low market value, such as the gypsum from the wet-scrubber technology of flue gas desulfurization, or combustion ash from fluidized bed combustion, which cause disposal problems. On the other hand,  $\text{SO}_2$  is an important raw material to produce a variety of chemicals in industries.  $\text{SO}_2$  utilization can be realized through three approaches: reduction, non-redox and oxidation reaction.

$\text{SO}_2$  can be converted to elemental sulfur through a reduction reaction. The most frequently used approach is called modified Claus process, which is a standard method for sulfur recovery in petroleum refining or chemical industries [15]. The recovered sulfur can be

used for the production of vulcanized rubber with a wide range of properties by varying the sulfur content.

Oxidation of  $\text{SO}_2$  is widely used for its utilization.  $\text{SO}_2$  can be converted to sulfuric acid for which there is a large demand. Through a contact process,  $\text{SO}_2$  is oxidized to  $\text{SO}_3$  followed with a  $\text{SO}_3$  absorption stage to produce fuming sulfuric acid. Sulfuric acid is the chemical produced in the largest amount in terms of mass, with an annual output of about 40 million tons in the United States. Many important chemicals are produced by using sulfuric acid as raw material. The sulfur containing fertilizers, such as superphosphate of lime and ammonium sulfate, use up to about 65 % of the sulfuric acid produced in United States.  $\text{SO}_2$  is often used as raw material by conversion to  $\text{SO}_3$  or sulfuric acid along with sodium chloride to produce sodium sulfate, an important chemical used in the manufacture of soap, paper and glass [16,17]. Fan *et al.* developed a low cost method to produce polymeric ferric sulfate (PFS) aiming at removing  $\text{SO}_2$  from flue gas in an economic way. PFS is an excellent coagulant for water and wastewater treatment, which features high efficiency and low corrosivity compared with other iron based coagulants [18,19].

The utilization of  $\text{SO}_2$  with non-redox method is relatively simple and direct. One of the typical chemicals produced with this method is sodium sulfite, which is generated by induction of  $\text{SO}_2$  to alkaline solution, such as sodium carbonate [20]. Sodium sulfite is mainly used as a pulping and reducing agent in paper industry, or a preservative agent for food and wine preparation. It is also be used as an ingredient in the cosmetic and soap formulations without causing healthy concern [21].

In view of the fact that  $\text{SO}_2$  has broad applications in industry, it is more environmentally and economically beneficial to take the approaches that use  $\text{SO}_2$  in the flue gas as feeding

stock to produce other valuable products, rather than those old methods that only focus on removing  $\text{SO}_2$  from flue gas. Based on this idea, two approaches that use  $\text{SO}_2$  in the flue gas were put forward and examined. In the first approach,  $\text{SO}_2$  was used to recover acetic acid and lactic acid from the biological process. The second approach converted  $\text{SO}_2$  to  $\text{SO}_3$  through oxidation with iron oxide ( $\text{Fe}_2\text{O}_3$ ) as catalyst, where the performance of microscale and nanoscale  $\text{Fe}_2\text{O}_3$  were compared and the kinetics models were established.

## 2. Dissertation Organization

This dissertation includes two published and one submitted papers, with “The recovery of acetic acid with sulfur dioxide” as Chapter 2, “The extraction of lactic acid with sulfur dioxide” as Chapter 3, and “Catalytic Oxidation of Sulfur Dioxide with Microscale and Nanoscale Iron Oxides as Catalysts” as Chapter 4. The dissertation begins with a general introduction as Chapter 1 and ends with a general conclusion as Chapter 5. Chapter 2 and Chapter 3 were published in *Biochemical Engineering Journal* in 2005. Chapter 4 was to be submitted to *Environmental Science and Technology*.

## 3. Literature Review

### 3.1. Recovery of Acetic Acid and Lactic Acid with $\text{SO}_2$

Having a history as old as the civilization, acetic acid nowadays plays an important role in various industrial applications. It is primarily used as a raw material in the manufacture of photographic films and polyethylene terephthalate (PET), a fully recyclable plastic. It also serves as a critical intermediate to facilitate many industrial processes, such as the manufacture of synthetic textile, adhesives and pharmaceutical products.

Although the food grade acetic acid is still produced with fermentation process, most acetic acid for industrial use is manufactured with a Monsanto process, in which carbon monoxide reacts with methanol at 180°C and pressures of 30~40 atm with rhodium complex as catalyst. The above process primarily relies on natural gas for raw material. The price of acetic acid is, consequently, intensively related to the natural gas price. Since natural gas is a non-regenerable resource and its reserve is limited, it is hardly able to support the acetic acid manufacture if acetic acid is still produced with the same process at the current consumption rate. As a result, the price increase of acetic acid will be inevitable due to the pressure from the rising cost of natural gas. The fermentation method, in this case, is economically advantageous since its feedstock is biomass, which is regenerable and of low cost.

Lactic acid is another important carboxylic acid that is widely demanded in diverse applications. It finds a variety of uses in food industry, where it is used as a flavor agent in the preparation of dairy products and fermented vegetables, a food additive for acidity adjustment, and the food preservative. Lactic acid is also applied in the pharmaceutical and cosmetic industry, and used as a feedstock to produce polylactic acid (PLA), a biodegradable thermoplastic polymer [22]. About half of lactic acid is produced through the fermentation of sugars, starch, or cheese whey in the presence of microorganisms such as *Lactobacillus delbrueckii* [23,24].

During the fermentation processes that produce either acetic acid or lactic acid, a pH decrease in the fermentation broth results from the acid accumulation in the system. The low pH has a negative effect on the bacteria that contribute to the acid production. If there is no acid removal from the system, the bacteria growth will be inhibited and the whole process is subject to failure.

Basically, the methods that are used to remove and recover the organic acids from the anaerobic system can be grouped into two categories, i.e., direct and indirect approaches. The typical direct separation method uses organic solvents and membrane methods for extracting organic acids [25,26]. Using this approach, the neutralization of the broth is not necessary and high concentrations of organic acids can be obtained with an additional distillation step. However, the separation can not be carried out continuously along with the fermentation process by using this approach. The amount of the broth that needs processing is considerably large in view of the fact that the concentrations of organic acids in the broth are rather low when a separation process is required.

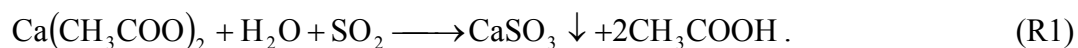
The indirect approach consists of two steps. The first step is to neutralize the fermentation broth with alkali materials, mostly calcium oxide and calcium hydroxide. With this step, the pH in the fermentation system is stabilized and the whole process is continued without affecting the metabolism of the bacteria. The second step of the indirect approach is the recovery of acetic acid or lactic acid from their salts, which are separated from the neutralized broth.

One of the efficient recovering methods of organic acids from their salt solutions is based on the extraction with organic solvents that are either water-soluble or insoluble. Urbas *et al.* reported that a water-soluble tertiary amine carbonate can react with calcium lactate to form calcium carbonate precipitate and water-soluble trialkylammonium lactate [27]. The calcium carbonate was then removed with a precipitation process, and the resulting liquid was heated to produce lactic acid and tertiary amine. Baniel *et al.* successfully realized the separation of lactate from the solution by using a water-immiscible trialkyl amine in the present of carbon dioxide [28]. The obtained mixture was composed of two phases, i.e., an organic phase

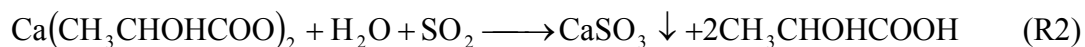
contained trialkyl-amine lactate salt and an aqueous phase contained either carbonate or bicarbonate. The organic phase was then back-extracted with water to recover lactic acid and the remaining trialkyl amine was recycled.

Another classical method to recover organic acids from their salt solutions is using strong acids, such as sulfuric acid to release acetic acid or lactic acid [29]. However, this method consumes expensive mineral acids and results in a mixture of saline and organic acids. To obtain commercial grade acetic acid or lactic acid, additional purification is needed after the acid addition. Since the solubility of calcium phosphate is very low [30], the use of phosphoric acid can avoid the salinity problem. But phosphoric acid is more expensive than sulfuric acid, thereby increasing the recovery costs. Some other approaches, such as ion exchange [31,32], and use of a membrane [29,33], were also tested for organic acid recovery from salt solution. But all these method encounter the high cost problem which prevents them from wide commercialization.

Instead of using a strong acid to recover acetic acid and lactic acid, a weak acid, sulfurous acid, is a promising alternative that leaves no salinity problem since the solubility of calcium sulfite is extremely low [30]. More important, using sulfurous acid is economically feasible since it originates from the dissolution of SO<sub>2</sub> in water. In practice, the recovery process can be realized by introducing SO<sub>2</sub> gas into the calcium lactate or calcium lactate solution to recover acetic acid or lactic acid. The reaction between organic calcium salts and SO<sub>2</sub> can be expressed as follows:



and



Because  $\text{SO}_2$  is widely available as an industrial byproduct [19,34], its use as a raw material for recovering organic acids is highly cost-effective. The proposed method avoids the need for expensive strong acids and the competition with other industries for resources. Its recovery principle is based on the chemical reaction and simple physical filtration, which means that it can be conducted at a much lower temperature than the conventional distillation methods. Therefore, it is especially attractive to industrial practice because it needs less energy and provides a safer separation environment. Since there are no studies on this method so far, this research was aimed at investigating the reaction between organic calcium salts and  $\text{SO}_2$ , the effect of temperature and  $\text{SO}_2$  flow rate on the reaction rate, and the acetic acid and lactic acid production rate.

### 3.2. Oxidation of $\text{SO}_2$ with Microscale and Nanoscale $\text{Fe}_2\text{O}_3$ as Catalysts

Among various approaches to use  $\text{SO}_2$ , the oxidation method is more economically feasible considering the diverse applications and rather huge demand for sulfate. As a major raw material,  $\text{SO}_2$  is used to produce sulfuric acid with a contact process in industry. At a temperature of about 450 °C, purified  $\text{SO}_2$  and air are mixed to form  $\text{SO}_3$  with the aid of a catalyst such as platinum or vanadium pentoxide. Based on this method, a similar catalytic oxidation process can be applied to the  $\text{SO}_2$  removal from flue gas. When using vanadium pentoxide, the conversion of  $\text{SO}_2$  is incomplete above the temperature of 420 °C, which is required for the contact process [35]. Research also showed that vanadium pentoxide is suspected of being a pulmonary carcinogen [36,37]. The use of precious metal catalyst, such as platinum, can avoid this problem, but this catalyst is very expensive and easy to be vitiated



by certain impurities in SO<sub>2</sub>. Therefore, a catalyst that is active at low temperature, more cost effective and environmental friendly is desirable to be used in flue gas cleaning process.

As an oxide from one of the first-row transition-metal, Fe<sub>2</sub>O<sub>3</sub> has outstanding electronic and magnetic properties, and is a less costly alternative to the currently used catalysts. It occurs naturally as the mineral hematite and is fairly active and selective for a number of heterogeneous catalytic reactions. By using activated carbon as the support material, Fe<sub>2</sub>O<sub>3</sub> is capable of oxidizing SO<sub>2</sub> in flue gas, where it acts as not only sorbent but also an effective catalyst [38]. It was also noticed that the removal of SO<sub>2</sub> by Fe<sub>2</sub>O<sub>3</sub> was enhanced by the presence of H<sub>2</sub>O and O<sub>2</sub> at the same time [39].

Compared with the non-nano metal oxides, the nanoscale metal oxides feature with a smaller particle size, higher specific surface area and greater concentration of catalytic active sites. These features make them more promising catalysts with significantly improved catalytic performance over non-nano catalysts. A nanoscale CeO<sub>2</sub>-supported Cr<sub>2</sub>O<sub>3</sub> catalyst was shown to be effective in the reduction of SO<sub>2</sub> from the flue gas with CO as a reducing agent [40]. In another application, a comparison was made between non-nano and nanoscale nickel oxide (NiO) on their ability on the ethane oxidative dehydrogenation activity. Results showed that temperature required for nanoscale NiO was lowered by about 125 °C when the same ethylene yield was obtained [41]

Extensive studies also have been made on the catalytic performance of nanoscale Fe<sub>2</sub>O<sub>3</sub>. By using nanoscale Fe<sub>2</sub>O<sub>3</sub> as a catalyst, Li *et al.* reported that CO can be removed efficiently through catalytic oxidation either in the presence or absence of O<sub>2</sub> [42]. It was shown that Fe<sub>2</sub>O<sub>3</sub> has two functions, both a catalyst of CO oxidation in the presence of O<sub>2</sub>, and, in absence of O<sub>2</sub>, as a direct SO<sub>2</sub> oxidant by losing the lattice oxygen. Nanoscale Fe<sub>2</sub>O<sub>3</sub> was also

successfully applied in catalytic conversion of phenolic and some aromatic compounds [43]. With the presence of nanoscale  $\text{Fe}_2\text{O}_3$  as a catalyst, it was found that the decomposition of these compounds was greatly enhanced at lowered temperatures due to the reduced activation energy.

On the basis of these facts, the performance of nanoscale  $\text{Fe}_2\text{O}_3$  in  $\text{SO}_2$  removing is also supposed to be promising. The main objective of this study, therefore, is to learn the efficiency of nanoscale  $\text{Fe}_2\text{O}_3$  on oxidizing  $\text{SO}_2$  into  $\text{SO}_3$ ; make comparison between microscale and nanoscale  $\text{Fe}_2\text{O}_3$  on their catalytic performance; and establish the kinetic models for oxidation reaction catalyzed by both microscale and nanoscale  $\text{Fe}_2\text{O}_3$ .

## References

- [1] H.F. Graf, J. Feichter, B. Langmann, Volcanic sulfur emissions: Estimates of source strength and its contribution to the global sulfate distribution, *J. Geophys. Res. (D Atmos.)* 102 (D9) (1997) 10727-10738.
- [2] M.J. Jaeger, D. Tribble, H.J. Wittig, Effect of 0.5 ppm sulfur dioxide on the respiratory function of normal and asthmatic subjects, *Lung* 156 (2) (1979) 119-127.
- [3] T.J. Witek, E.N. Schachter, G.J. Beck, W.S. Cain, G. Colice, B.P. Leaderer, Respiratory symptoms associated with sulfur dioxide exposure, *Int. Arch. Occup. Environ. Health* 55 (2) (1985) 179-183.
- [4] P.T. Radulovic, L.D. Smoot, Coal processes and technologies, *Coal Sci. Technol.* 20 (Fundamentals of Coal Combustion for Clean and Efficient Use) (1993) 1-77.

- [5] C. Brereton, Combustion performance, Circulating Fluidized Beds, (1997) 369-416.
- [6] J. Kaminski, Technologies and costs of SO<sub>2</sub>-emissions reduction for the energy sector, Appl. Energy 75 (3-4) (2003) 165-172.
- [7] J. Warych, M. Szymanowski, Model of the wet limestone flue gas desulfurization process for cost optimization, Ind. Eng. Chem. Res. 40 (12) (2001) 2597-2605.
- [8] H. Namba, O. Tokunaga, S. Hashimoto, T. Tanaka, Y. Ogura, Y. Doi, S. Oaki, M. Izutsu, Pilot-scale test for electron beam purification of flue gas from coal-combustion boiler, Radiat. Phys. Chem. 46 (4-6, Proceedings of the 9th International Meeting on Radiation Processing, 1994, Pt. 2) (1995) 1103-1106.
- [9] Y.S. Mok, H.W. Lee, Y.J. Hyun, Flue gas treatment using pulsed corona discharge generated by magnetic pulse compression modulator, J. Electrostatics 53 (3) (2001) 195-208.
- [10] E.M. Van Veldhuizen, L.M. Zhou, W.R. Rutgers, Combined effects of pulsed discharge removal of NO, SO<sub>2</sub>, and NH<sub>3</sub> from flue gas, Plasma Chem. Plasma Proc. 18 (1) (1998) 91-111.
- [11] Y. Zhu, J.O. Chae, K.Y. Kim, K.O. Kim, Y.K. Park, Effects of water vapor and ammonia on SO<sub>2</sub> removal from flue gases using pulsed corona discharge, Plasma Chem. Plasma Proc. 22 (1) (2002) 187-195.

- [12] K. Onda, Y. Kasuga, K. Kato, M. Fujiwara, M. Tanimoto, Electric discharge removal of SO<sub>2</sub> and NO<sub>x</sub> from combustion flue gas by pulsed corona discharge, *Energy Convers. Manage.* 38 (10-13) (1997) 1377-1387.
- [13] L. Alonso, J.M. Palacios, R. Moliner, The performance of some ZnO-based regenerable sorbents in hot coal gas desulfurization long-term tests using graphite as a pore-modifier additive, *Energy Fuels* 15 (6) (2001) 1396-1402.
- [14] R.B. Slimane, J. Abbasian, Copper-based sorbents for coal gas desulfurization at moderate temperatures, *Ind. Eng. Chem. Res.* 39 (5) (2000) 1338-1344.
- [15] A.A. Davydov, V.I. Marshneva, M.L. Shepotko, Metal oxides in hydrogen sulfide oxidation by oxygen and sulfur dioxide I. The comparison study of the catalytic activity. Mechanism of the interactions between H<sub>2</sub>S and SO<sub>2</sub> on some oxides, *Appl. Catal. A Gen.* 244 (1) (2003) 93-100.
- [16] S. Stankowski, A. Murkowski, R. Malinowski, Possibilities of utilization of a byproduct from removing SO<sub>2</sub> and NO<sub>x</sub> from flue gases as a nitrogen-sulfur fertilizer, *Folia Univ. Agric. Stetin.* 190 (1998) 277-281.
- [17] J.A.B. Satrio, S.B. Jagtap, T.D. Wheelock, Utilization of sulfur oxides for the production of sodium sulfate, *Ind. Eng. Chem. Res.* 41 (15) (2002) 3540-3547.
- [18] M. Fan, R.C. Brown, S.W. Sung, Y. Zhuang, A process for synthesizing polymeric ferric sulfate using sulfur dioxide from coal combustion, *Proceedings - Annual International Pittsburgh Coal Conference 17th* (2000) 2222-2229.

- [19] A.D. Butler, M. Fan, R.C. Brown, A.T. Cooper, J.H. van Leeuwen, S. Sung, Absorption of dilute SO<sub>2</sub> gas stream with conversion to polymeric ferric sulfate for use in water treatment, *Chem. Eng. J.* 98 (3) (2004) 265-273.
- [20] I.G. Blyakher, M.M. Vaisbein, I.S. Chernyi, Dry process for obtaining anhydrous sodium sulfite, *Khim. Prom.* 47 (9) (1971) 679-81.
- [21] F.A. Andersen, Final report on the safety assessment of sodium sulfite, potassium sulfite, ammonium sulfite, sodium bisulfite, ammonium bisulfite, sodium metabisulfite, and potassium metabisulfite, *Int. J. Toxicol.* 22 (Suppl. 2) (2003) 63-88.
- [22] N. Narayanan, P.K. Roychoudhury, A. Srivastava, L-(+)-lactic acid fermentation and its product polymerization, *Electron. J. Biotechnol.* 7 (2) (2004) No pp. given.
- [23] D.M. Bai, M.Z. Jia, X.M. Zhao, R. Ban, F. Shen, X.G. Li, S.M. Xu, L-(+)-lactic acid production by pellet-form *Rhizopus oryzae* R1021 in a stirred tank fermentor, *Chem. Eng. Sci.* 58 (3-6) (2003) 785-791.
- [24] C.H. Holten, A. Mueller, D. Rehbinder, Lactic acid. Properties and chemistry of lactic acid and derivatives, Verlag Chemie, Weinheim, Germany, 1971.
- [25] A. Shishikura, H. Kimbara, K. Yamaguchi, K. Arai, Process for recovering high-purity organic acids, *Eur. Pat. Appl.* 91116375.6 (1992).
- [26] T. Sano, S. Eijiri, M. Hasegawa, Y. Kawakami, N. Enomoto, Y. Tamai, H. Yanagishita, Silicate membrane for separation of acetic acid/water mixture, *Chem. Lett.* (2) (1995) 153-154.

- [27] B. Urbas, Recovery of organic acids from a fermentation broth, U.S. Patent 4,444,881 (1984).
- [28] A.M. Baniel, A.M. Eyal, J. Mizrahi, B. Hazan, R.R. Fisher, J.J. Kolstad, B.F. Stewart, Lactic acid production, separation and/or recovery process, U.S. Patent 6,187,951 (2001).
- [29] N.A. Collins, M.R. Shelton, G.W. Tindall, S.T. Perri, R.S. O'meadhra, C.W. Sink, B.K. Arumugam, J.C. Hubbs, Process for the recovery of organic acids from aqueous solutions, U.S. Patent 6,670,505 (2003).
- [30] D.R. Lide, CRC Handbook of Chemistry and Physics, 84th Ed., CRC Press, Boca Raton, FL, 2003.
- [31] R.A. Yates, Removal and concentration of lower molecular weight organic acids from dilute solutions, U.S. Patent 4,282,323 (1981).
- [32] A. Baniel, A process for the recovery of dicarboxylic acids from solutions containing their salts using carbon dioxide and anion exchangers, PCT Int. Appl. PCT/GB97/01811, 1998.
- [33] M.C.M Cockrem, Process for recovering organic acids from aqueous salt solutions, U.S. Patent 5,522,995 (1996).
- [34] M. Fan, R.C. Brown, Y. Zhuang, A.T. Cooper, M. Nomura, Reaction kinetics for a novel flue gas cleaning technology, Environ. Sci. Technol. 37 (7) (2003) 1404-1407.

- [35] J.P. Dunn, H.G. Stenger, I.E. Wachs, Molecular structure-reactivity relationships for the oxidation of sulfur dioxide over supported metal oxide catalysts, *Catal. Today* 53 (4) (1999) 543-556.
- [36] N.B. Ressa, B.J. Chou, R.A. Renne, J.A. Dill, R.A. Miller, J.H. Roycroft, J.R. Hailey, J.K. Haseman, J.R. Bucher, Carcinogenicity of inhaled vanadium pentoxide in F344/N rats and B6C3F1 mice, *Toxicol. Sci.* 74 (2) (2003) 287-296.
- [37] L. Zhang, A.B. Rice, K. Adler, P. Sannes, L. Martin, W. Gladwell, J.S. Koo, T.E. Gray, J.C. Bonner, Vanadium stimulates human bronchial epithelial cells to produce heparin-binding epidermal growth factor-like growth factor: a mitogen for lung fibroblasts, *Am. J. Respir. Cell Mol. Biol.* 24 (2) (2001) 123-131.
- [38] H.H. Tseng, M.Y. Wey, Y.S. Liang, K.H. Chen, Catalytic removal of SO<sub>2</sub>, NO and HCl from incineration flue gas over activated carbon-supported metal oxides, *Carbon* 41 (5) (2003) 1079-1085.
- [39] J. Ma, Z. Liu, S. Liu, Z. Zhu, A regenerable Fe/AC desulfurizer for SO<sub>2</sub> adsorption at low temperatures, *Appl. Catal. B Environ.* 45 (4) (2003) 301-309.
- [40] C.L. Chen, H.S. Weng, Nanosized CeO<sub>2</sub>-supported metal oxide catalysts for catalytic reduction of SO<sub>2</sub> with CO as a reducing agent, *Appl. Catal. B Environ.* 55 (2) (2005) 115-122.

- [41] Y. Wu, T. Chen, X.D. Cao, W.Z. Weng, J.F. Zhang, H.L. Wan, Comparison study of large and nano-size NiO for oxidative dehydrogenation of ethane to ethylene, *Huaxue Xuebao* 62 (18) (2004) 1678-1682.
- [42] P. Li, D.E. Miser, S. Rabiei, R.T. Yadav, M.R. Hajaligol, The removal of carbon monoxide by iron oxide nanoparticles, *Appl. Catal. B Environ.* 43 (2) (2003) 151-162.
- [43] E.J. Shin, D.E. Miser, W.G. Chan, M.R. Hajaligol, Catalytic cracking of catechols and hydroquinones in the presence of nano-particle iron oxide, *Appl. Catal. B Environ.* 61 (1-2) (2005) 79-89.



**CHAPTER 2. THE RECOVERY OF ACETIC ACID WITH SULFUR DIOXIDE**

A paper published in *Biochemical Engineering Journal*<sup>1</sup>

Yonghui Shi<sup>2</sup>, Maohong Fan<sup>2,\*</sup>, Na Li<sup>2</sup>, Robert C. Brown<sup>2</sup> and Shihwu Sung<sup>3</sup>

<sup>1</sup>Reprinted from *Biochemical Engineering Journal*, 22(3), 207-210, 2005, with permission from Elsevier.

<sup>2</sup>Center for Sustainable Environmental Technologies, Iowa State University, Ames, IA, 50011, U.S.A.

<sup>3</sup>Department of Civil, Construction and Environmental Engineering, Iowa State University, Ames, IA, 50011, U.S.A.

**Abstract**

This paper studies the reaction between SO<sub>2</sub> and calcium acetate, which potentially can be used to recover acetic acid from the anaerobic fermentation broth of a SO<sub>2</sub> waste stream. The conversion of given amounts of calcium acetate to acetic acid was evaluated under different reaction temperatures and flow rates of SO<sub>2</sub>. Analyses of concentrations of the produced acetic acid indicated that the reactions between SO<sub>2</sub> and calcium acetate were complete under all experimental conditions.

*Keywords:* Acetic acid; Calcium acetate; Mixing; Separation; Sulfur dioxide; Waste treatment

---

\*Corresponding author: e-mail: fan@ameslab.gov, phone: (515) 294-3951, fax: (515) 294-3091

## 1. Introduction

Acetic acid is an important industrial chemical, about 7.835 billion pounds of which was produced in the United States in 2002. As one of the most widely used carboxylic acids, it is often used as a raw material to prepare other valuable products such as acetic esters. Another important application of acetic acid is to serve as a solvent to facilitate many industrial processes, such as the manufacture of cellulose acetate and pharmaceutical products.

Acetic acid produced today is primarily based on natural gas [1]. However, as a nonrenewable resource, and at current high rates of consumption, natural gas is barely able to support the acetic acid industry. It is anticipated that, unless other production methods are successfully developed, the price of acetic acid will increase markedly in the future. As a promising alternative, the production of acetic acid using biomass materials recently gains more interest primarily attributed to its cost-effectiveness. However, the main obstacle to widespread use of this method is the difficulty of separating acetic acid from an anaerobic system or waste streams from biological processes. To alleviate the negative effects of acid accumulation, the generated acid must be either removed or neutralized. Methods used for the separation of acetic acid from anaerobic systems can be divided into two categories: viz. direct and indirect approaches. The typical direct separation method uses organic solvents and membrane methods for extracting organic acids [2, 3]. Indirect approaches involve two steps. The first step of the indirect method uses alkali materials, mostly calcium oxide and calcium hydroxide, to neutralize the acetic acid in broth and separate the resulting acetate, providing an appropriate environment in which bacteria may survive. The second step in the indirect method is to regenerate acetic acid from the acetate separated from the broth.

Various approaches have been explored for this step, including ion exchange [4, 5], acidification by strong mineral acids (e.g. hydrochloric, sulfuric, or phosphoric acid), and use of a membrane [6]. There is no doubt that each of these approaches has its merits. However, all must address the same high cost problems before they can be successfully commercialized.

This research studies the use of SO<sub>2</sub> to recover acetic acid from calcium acetate resulting from the neutralization process of waste stream containing acetic acid. The reaction between calcium acetate and SO<sub>2</sub> can be expressed as follows:



There are several advantages in this acetic acid separation process. Firstly, it does not need expensive chemicals. SO<sub>2</sub> is widely available as a byproduct of many industries [7, 8].

Secondly, it can be conducted with a temperature lower than that needed for conventional azeotropic distillation and simple distillation. Therefore, it needs less energy and provides safer separation environments. Finally, CaO-SO<sub>2</sub> acetic acid separation approach is a green one because they are available from the decomposition of calcium sulfite obtained from the

Reaction R1. Since its standard-state Gibbs function change,  $\Delta G_T^0$ , is  $-126.72 \text{ kJ} \cdot \text{mol}^{-1}$  [9, 10], the thermodynamic calculation shows that R1 is feasible [11]. An equilibrium constant

K at the standard state,  $1.6 \times 10^{22}$ , can also be calculated based on the formula of

$\Delta G_T^0 = -RT \ln K$ . However, the calculated feasibility needs to be tested experimentally. This research focuses on whether R1 can be completed under different reaction conditions.

## 2. Materials and Methods

### 2.1. Materials

Calcium acetate (99.8%) and sulfur dioxide (anhydrous, 99.98%) used in this research was purchased from Fisher Scientific International Inc. and Matheson Tri-Gas Inc. (Montgomeryville, PA), respectively.

### 2.2. Apparatus and Operational Procedures

A 500 mL reactor (Chemglass, Inc., Vineland, NJ) was used to conduct all experiments. Temperature control was realized using a Neslab RTE-111 bath/circulator, which circulated a low-temperature oil (Ace Glass, Inc., Vineland, NJ) through the jacket of the reactor. To avoid water loss through evaporation, the outlet gas from the reactor passed through a condenser that was maintained at approximately 3 °C by a heated/refrigerated Cole Parmer Polystat<sup>®</sup> 6-liter circulator unit. The inlet and outlet concentrations of SO<sub>2</sub> in the gas stream were monitored using a California Analytical model ZRF NDIR gas analyzer (manufactured by Fuji Electric Company, Saddle Brook, NJ). The gas analyzer reads 0 to 10 v% SO<sub>2</sub> by 0.01 % and has a repeatability of  $\pm 0.5$  % of full scale. The SO<sub>2</sub> readings of the gas analyzer were recorded with a computer-based data collection system every 10 seconds for further analysis. During the experiments, the reaction mixture in the reactor was stirred at 60 rpm for all trials by an adjustable overhead stirrer connected to a Teflon mixer. Mass measurements of the calcium acetate and water were made on a Mettler model PM4000 balance with a linearity of  $\pm 0.02$  g. The flow rates of gases were controlled with flow meters. Reaction

temperature was measured with a non-mercury glass thermometer inserted into the reaction mixture.

The first step of the reaction was to add 40.0 g  $\text{Ca}(\text{CH}_3\text{COO})_2 \cdot \text{H}_2\text{O}$  into a reactor filled with 245.5 g deionized water and then to stir the mixture continuously at 60 rpm for 30 minutes to completely dissolve all of the added calcium acetate. Since the final concentration of acetic acid generated for all tests was set to be 1.667 M, the quantities of calcium acetate and water added in each test were the same.  $\text{N}_2$  and  $\text{SO}_2$  were then sparged into the reactor solution through an 8 mm glass tube to start the reaction. The  $\text{SO}_2$  gas analyzer was calibrated before and after each test run. The calibrations were performed with known concentrations of standard gases supplied by BOC Gases, Des Moines, Iowa. Each experiment was ended when the outlet concentration of  $\text{SO}_2$  was the same as the inlet concentration.

Variables used in this research include reaction temperature and concentration of  $\text{SO}_2$  in the gas stream, with a total flow rate of 3447.0 mL/min. The reaction temperature varied from 20 to 60 °C, with an interval of 10 °C. The concentration of  $\text{SO}_2$  in the gas mixture varied from 3.0 to 9.0 v%, with an interval of 1.5 v%.

### *2.3. Analysis of Acetic Acid with HPLC.*

The acetic acid produced from R1 was analyzed with a Waters 501 high-performance liquid chromatograph (HPLC). The organic acid analysis column used was provided by Alltech Prevail (Alltech Associates, Inc). The material used in mobile phase was a degassed  $\text{KH}_2\text{PO}_4$  solution (0.005 M). The HPLC operation parameters during the measurements of

acetic acid include: 1) 192 nm of UV light, 2) a column pressure of 900 psi, and 3) a mobile phase flow rate of 0.8 mL/min.

### 3. Results and Discussion

Once sulfur dioxide was sparged into the calcium acetate solution, it underwent a series of steps before reacting with the calcium acetate, including gas phase diffusion, mass transfer at the gas-liquid interface, hydrolysis and ionization of the dissolved  $\text{SO}_2$ , and aqueous diffusion and reaction between the calcium acetate and sulfurous acid. The solubility of  $\text{SO}_2$  in 100.0 g water is 10.6 g at a temperature of 20 °C and 3.2 g at 60 °C [11], which means that the quantity of  $\text{SO}_2$  dissolved in water is considerable given enough time. However, the rate of  $\text{SO}_2$  dissolved into water was so slow that the  $\text{SO}_2$  concentration difference in the inlet and outlet stream was negligible when only water existing in the reaction vessel. After addition of calcium acetate in the water, the experiment showed that the  $\text{SO}_2$  concentrations in the outlet stream remained at zero throughout the process. This suggested that the solution's capacity for absorption of  $\text{SO}_2$  was greatly increased by the dissolution of calcium acetate. When  $\text{SO}_2$  was dissolved into the solution containing calcium acetate, it reacted to yield  $\text{HSO}_3^-$  and  $\text{SO}_3^{2-}$ , thereby lowering the dissolved  $\text{SO}_2$  concentration and allowing more total  $\text{SO}_2$  from the gas phase to be dissolved [12].

The solubility of  $\text{Ca}(\text{CH}_3\text{COO})_2$  in 100.0 g of water is 37.4 g at a temperature of 0 °C and 29.7 g at 100 °C [13]. Under experimental conditions, the added calcium acetate was completely dissolved. The produced calcium sulfite, however, had a very low solubility in water: 0.0043 g at 18 °C and 0.0011 g at 100 °C in 100.0 g water [13]. When  $\text{SO}_2$  was sparged into the solution, it dissolved in the water and reacted with calcium acetate to

produce calcium sulfite precipitate and acetic acid. Calcium sulfite was separated from the liquid with a simple filtration process.

In the experimental design, the assumption was made that the reaction endpoint would be reached when concentrations of  $\text{SO}_2$  in the inlet and outlet mixture gases were identical. At the beginning of the reaction,  $\text{SO}_2$  in the outlet gas from the reactor was nondetectable, indicating that the  $\text{SO}_2$  in the gas mixture was completely removed by the reaction. With the proceeding of reaction and consumption of calcium acetate, the remaining calcium acetate concentration in the reactor was not high enough to remove the introduced  $\text{SO}_2$  instantly, thus leading to the increase of  $\text{SO}_2$  concentration in the outlet gas. The time at which  $\text{SO}_2$  began to appear in the outlet gas was referred as breakthrough point. At the end of reaction,  $\text{SO}_2$  was no longer consumed and dissolved into the solution. Its concentration in the outlet gas was therefore the same as that in the inlet gas.

The relationships between reaction temperature and the reaction time needed for the completion of reactions at given conditions are shown in Figure 1. Figure 1 demonstrates that the higher the reaction temperature is the shorter the reaction time needed. This fact can be explained with kinetic theory that higher temperature results in a higher reaction rate constant. It can be seen that the reaction time at the temperature of  $60\text{ }^\circ\text{C}$  was only about 75 % of that at  $20\text{ }^\circ\text{C}$  with the  $\text{SO}_2$  concentration of 9 v%. Figure 1 also shows that the breakthrough points at a temperature of  $60\text{ }^\circ\text{C}$  were about 75 % of those at  $20\text{ }^\circ\text{C}$ .

$\text{SO}_2$  concentrations also directly affected reaction times. Higher  $\text{SO}_2$  concentrations shortened the amount of time needed to complete reactions in the system. Figure 1 indicates that reaction time decreased as the  $\text{SO}_2$  flow rate increased—an obvious outcome, since the higher  $\text{SO}_2$  concentrations represent that more  $\text{SO}_2$  was sparged into the system over the

same period. However, the reaction time was not proportional to the flow rate at which SO<sub>2</sub> was sparged into the system. The results demonstrate that reaction times under the condition of 3.0 v% of SO<sub>2</sub> concentration were only about 50 % greater than those with a concentration of 9.0 v%, assumed previously to be up to 200 % greater if SO<sub>2</sub> concentrations determined reaction time. On the other hand, the results from Figure 1 show that breakthrough points under the condition of 3.0 v% of SO<sub>2</sub> concentration were only about 80 % greater than those with a concentration of 9.0 v%. This indicates that reaction in the system was complex, and that the reaction rate was not controlled solely by means of the SO<sub>2</sub> flow rate.

Considering the yield of the reaction, which is the ratio between SO<sub>2</sub> changed to the calcium sulfite and the SO<sub>2</sub> addition to the reactor, the best reaction conditions include the SO<sub>2</sub> concentration of 3 v% and the temperature of 60 °C. For industrial application, it is desirable to completely remove SO<sub>2</sub> from the inlet gas, which is corresponding to the period before the breakthrough point. The experimental results indicates that the amount of SO<sub>2</sub> introduced into the system and converted to CaSO<sub>3</sub> before the breakthrough point was about 85 % of that required for complete conversion of calcium acetate at the temperature of 20 °C, despite the SO<sub>2</sub> concentration in the inlet gas. This fact shows that a reaction condition of room temperature and higher SO<sub>2</sub> concentration may be used in the industrial application.

The concentrations of acetic acids produced under different reaction conditions are listed in the Table 1. It shows that SO<sub>2</sub> concentration and reaction temperature had no substantial effect on the concentrations of acetic acid produced. Although there were some deviations from the designed 1.667 M of acetic acid concentration, these differences were random and no indication of effects from these two factors could be found. This result suggests that high concentrations of SO<sub>2</sub> can be used to recover acetic acid from the calcium acetate solution at



room temperature. Since reaction at room temperature would save large amounts of the energy needed to heat for reaction, both of these conditions are highly desirable in real-world industrial applications, albeit at the cost of longer reaction times. Increasing  $\text{SO}_2$  concentrations, however, can make up this deficiency. Large amount of gas stream containing high concentration of  $\text{SO}_2$  is available in new generation of power plants [14, 15], which will make the recovery of acetic acid from biostreams with  $\text{SO}_2$  feasible.

#### **4. Conclusions**

Sulfur dioxide can be used to recover acetic acid efficiently from calcium acetate solutions. The experimental results show that the time required for a complete reaction decreases with an increase of reaction temperature and  $\text{SO}_2$  flow rate. Although a change of reaction conditions leads to a change of reaction time, analysis of the produced acetic acid concentrations demonstrates that the complete conversion of calcium acetate to acetic acid was not affected. This suggests that the recovery process can be designed using a higher  $\text{SO}_2$  flow rate at room temperature without affecting recovery efficiency. Since energy for heating is substantially reduced, the latter feature is economically attractive for the industrial recovery of acetic acid from biological fermentation broth. Industry can either increase the flow rate of  $\text{SO}_2$  containing gas or even use pure  $\text{SO}_2$  gas. The findings of this study indicate that recovering acetic acid with  $\text{SO}_2$  is applicable.

#### **Acknowledgement**

This research was funded by USDA. In addition, the authors thank Ms. Desi Gunning of the Department of Biochemistry, Biophysics, and Molecular Biology at ISU for her assistance in performing HPLC tests.

**References**

- [1] V.H. Agreda, J.R. Zoeller, Acetic acid and its derivatives, Marcel Dekker, Inc., New York, 1993.
- [2] A. Shishikura, H. Kimbara, K. Yamaguchi, K. Arai, Process for recovering high-purity organic acids, Eur. Pat. Appl. 91116375.6, 1992.
- [3] T. Sano, S. Eijiri, M. Hasegawa, Y. Kawakami, N. Enomoto, Y. Tamai, H. Yanagishita, Silicate membrane for separation of acetic acid/water mixture, Chem. Lett. 2 (1995), 153-154.
- [4] R.A. Yates, Removal and concentration of lower molecular weight organic acids from dilute solutions, U.S. Pat. 4282323, 1981.
- [5] A. Baniel, A process for the recovery of dicarboxylic acids from solutions containing their salts using carbon dioxide and anion exchangers, PCT Int. Appl. PCT/GB97/01811, 1998.
- [6] M.C.M. Cockrem, Process for recovering organic acids from aqueous salt solutions, U.S. Pat. 5522995, 1996.
- [7] A.D. Butler, M. Fan, R.C. Brown, A.T. Cooper, J. H. van Leeuwen, S. Sung, Absorption of dilute SO<sub>2</sub> gas stream with conversion to polymeric ferric sulfate for use in water treatment, Chem. Eng. J. 98 (2004) 265-273.

- [8] M. Fan, R.C. Brown, Y. Zhuang, A.T. Cooper, M. Nomura, Reaction kinetics for a novel flue gas cleaning technology, *Environ. Sci. Technol.* 37 (2003) 1404-1407.
- [9] Shanghai Normal University, Hebei Normal University, Central China Normal University, South China Normal University and Xinxiang Normal College, *Physical chemistry*, 2nd ed., Higher Education Press, Beijing, China, 1985.
- [10] H. Li, Research on sulfur recovery from flue gas desulfurization gypsum by catalytical reducing, Ph. D. Thesis, Chinese Academy of Sciences, China, 1999.
- [11] D.R. Lide, *CRC handbook of chemistry and physics*, 84th ed., CRC, Boca Raton, Florida, 2003.
- [12] S.E. Schwartz, J.E. Freiberg, Mass-transport limitation to the rate of reaction of gases in liquid droplets: application to oxidation of sulfur dioxide in aqueous solutions, *Atmos. Environ.* 15 (1981) 1129-1144.
- [13] R.C. Weast, *CRC handbook of chemistry and physics*, 64th ed., 1984.
- [14] A. Durych, D.L. Wise, Y.A. Levendis, M. Metghalchi, *Industrial chemistry library*, Vol. 2: Calcium magnesium acetate. An emerging bulk chemical for environmental applications, Elsevier, Amsterdam, Netherlands, 1991.
- [15] H. Yoon, Flue gas desulfurization process, U.S. Pat. 4615871, 1986.

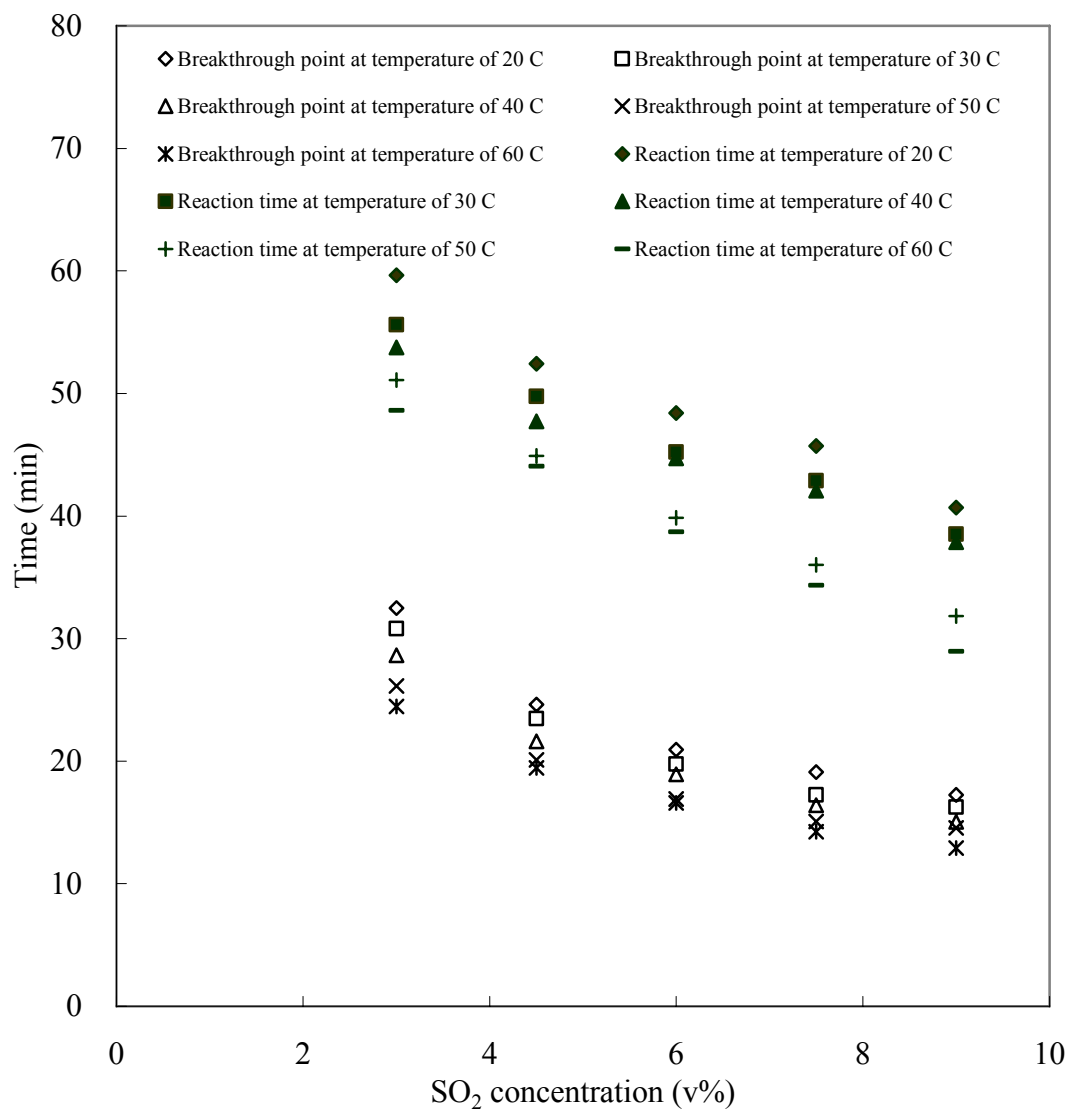


Fig. 1. The effect of SO<sub>2</sub> concentration and reaction temperature on the reaction rate  
(Total flowrate of N<sub>2</sub> and SO<sub>2</sub> mixture was 3447.0 mL/min)

Table 1. The concentrations of produced acetic acid (M) under different experimental conditions

Temperature (°C) \ SO <sub>2</sub> Concentration (v %)	20	30	40	50	60
3.0	1.636 ± 0.030	1.561 ± 0.017	1.606 ± 0.024	1.671 ± 0.012	1.629 ± 0.026
4.5	1.666 ± 0.012	1.721 ± 0.029	1.624 ± 0.049	1.702 ± 0.029	1.658 ± 0.036
6.0	1.669 ± 0.050	1.650 ± 0.053	1.661 ± 0.055	1.665 ± 0.035	1.666 ± 0.008
7.5	1.658 ± 0.013	1.692 ± 0.029	1.679 ± 0.063	1.658 ± 0.013	1.647 ± 0.012
9.0	1.673 ± 0.009	1.666 ± 0.023	1.645 ± 0.010	1.695 ± 0.038	1.571 ± 0.003

### CHAPTER 3. THE EXTRACTION OF LACTIC ACID WITH SULFUR DIOXIDE

A paper published in *Biochemical Engineering Journal*<sup>1</sup>

Yonghui Shi<sup>2</sup>, Maohong Fan<sup>2,\*</sup>, Ming Xu<sup>2</sup>, Robert C. Brown<sup>2</sup> and J(Hans) van Leeuwen<sup>3</sup>

<sup>1</sup>Reprinted from *Biochemical Engineering Journal*, 24(2), 157-160, 2005, with permission from Elsevier.

<sup>2</sup>Center for Sustainable Environmental Technologies, Iowa State University, Ames, IA, 50011, U.S.A.

<sup>3</sup>Department of Civil, Construction and Environmental Engineering, Iowa State University, Ames, IA, 50011, U.S.A.

#### Abstract

This paper studies the reaction between SO<sub>2</sub> and calcium lactate, which potentially can be used to recover lactic acid from the anaerobic fermentation broth of an SO<sub>2</sub> waste stream. The conversion of given amounts of calcium lactate to lactic acid was evaluated under different reaction temperatures and flow rates of SO<sub>2</sub>. Analyses of concentrations of the produced lactic acid indicated that the reactions between SO<sub>2</sub> and calcium lactate were complete under all experimental conditions.

*Keywords:* Lactic acid; calcium lactate; mixing; separation; sulfur dioxide; waste treatment

---

\*Corresponding author: e-mail: fan@ameslab.gov, phone: (515) 294-3951, fax: (515) 294-

3091

## 1. Introduction

Used widely in food and pharmaceutical manufacturing, lactic acid can also be used for the production of valuable biodegradable polymers, thus creating increased demand for it. Industrial lactic acid is produced primarily through the fermentation of sugars, starch, or cheese whey in the presence of microorganisms such as *Lactobacillus delbrueckii* [1]. The production of lactic acid by fermentation results in a decrease in the pH of the broth. The resulting higher acidity inhibits bacterial growth. To avoid the negative effects of decreasing pH, the accumulated lactic acid must either be neutralized or removed from the broth. The hydroxides, carbonates, or bicarbonates of alkali metals are commonly added to the fermentation broth to neutralize the produced acid. As the most economical bases are calcium carbonate or calcium hydroxide, the principal form of the lactate in the fermentation broth is calcium lactate.

Extensive research has been conducted to develop methods for producing lactic acid from a calcium lactate solution that are both effective and economical. One of most common methods is to extract lactic acid using either water-soluble or insoluble organic solvents. One reportedly effective extractant is a water-soluble tertiary amine carbonate [2] that reacts with calcium lactate to form calcium carbonate precipitate and water-soluble trialkylammonium lactate. After removal of the precipitates, the remaining solution is heated to obtain lactic acid and tertiary amine. By adding a water-immiscible trialkyl amine to a lactate solution in the presence of carbon dioxide, Baniel et al. [3] obtained a two-phase system in which the organic phase contained trialkyl-amine lactate salt and the aqueous phase contained either carbonate or bicarbonate. The organic phase was then back-extracted with water to recover

lactic acid and the remaining trialkyl amine was recycled. Another approach is to use mineral acids such as hydrochloric acid or sulfuric acid to recover lactic acid from lactate salt solutions [4]. However, this method consumes expensive mineral acids and results in saline lactic acid solutions, thereby increasing recovery costs. Because calcium phosphate is not very soluble, the use of phosphoric acid could avoid the salinity problem. However, this is a more expensive option.

The research outlined in this paper investigates the use of sulfurous acid to recover lactic acid, since the solubility of calcium sulfite is very low. In practice, sulfurous acid is formed by dissolving sulfur dioxide (SO<sub>2</sub>) gas into the calcium lactate solution to recover lactic acid (R1). The calcium sulfite can be easily precipitated and separated from the lactic acid solution, i.e.:



Because SO<sub>2</sub> is a widely available industrial byproduct and often a nuisance waste in flue gases [5, 6], its use as a raw material for recovering lactic acid is highly cost-effective. Also, by converting waste gas into a useful raw material, SO<sub>2</sub> does not compete with other industrial applications for mineral acid resources. In view of these advantages, sulfur dioxide may provide a promising lactic acid recovery approach. As there have been no detailed studies of this method to date, this paper investigates the reaction between calcium lactate and SO<sub>2</sub>, the effects of temperature and SO<sub>2</sub> flow rate on the reaction rate, and the lactic acid production rate.



## 2. Materials and Methods

### 2.1. Reagents

The calcium lactate  $\text{Ca}(\text{CH}_3\text{CHOHCOO})_2 \cdot 5\text{H}_2\text{O}$ , compressed nitrogen gas, and sulfur dioxide (anhydrous, 99.98%) used in this research was purchased from Fisher Scientific International Inc., Linweld Inc. (Des Moines, IA), and Matheson Tri-Gas Inc. (Montgomeryville, PA), respectively.

### 2.2. Apparatus

A 500 mL jacketed glass reaction vessel (Chemglass, Inc., Vineland, NJ) was used in the experiment. To keep the temperature constant within the vessel, a low-temperature silicone oil (Ace Glass, Inc., Vineland, NJ) was circulated through the jacket using an alternately heated and refrigerated Neslab RTE-111 circulator. The outlet gas from the reactor was measured with a California Analytical model ZRF NDIR gas analyzer (Fuji Electric Company, Saddle Brook, NJ). The analyzer also sent a DC signal to a connected computer system that recorded the  $\text{SO}_2$  concentration. In each experimental trial, the inlet  $\text{SO}_2$  concentration was verified at the beginning of the reaction with the gas analyzer for use in subsequent removal efficiency calculations. For all experiments, the reaction mixture was stirred with an adjustable overhead stirrer connected to an impeller. The nitrogen ( $\text{N}_2$ ) and  $\text{SO}_2$  mixture gas was introduced into the reactor through an 8 mm glass tube, and the reaction temperature was measured with a mercury thermometer inserted into the reaction mixture.

### 2.3. Operational Procedures

The first step of the reaction involved the addition of 40.0 g  $\text{Ca}(\text{CH}_3\text{CHOHCOO})_2 \cdot 5\text{H}_2\text{O}$  into a reactor containing 201.0 g deionized water, which was mixed continuously at 60 rpm for 30 minutes. This step formed a saturated calcium lactate solution with a temperature equilibrated with that of the silica oil in the jacket, which in turn was set by the circulator. After mixing, the mixture gas of  $\text{N}_2$  and  $\text{SO}_2$  was introduced into the solution at a constant flow rate. In order to eliminate any interference caused by differing gas flows in the various trials, the total flow of  $\text{N}_2$  and  $\text{SO}_2$  was controlled with a rotameter at a constant rate during the entire reaction. By this means, the  $\text{SO}_2$  flow rate could be changed without affecting reaction conditions. The experiment was stopped when the outlet  $\text{SO}_2$  concentration reached the same level as that in the inlet stream.

The effect of the  $\text{SO}_2$  flow rate and temperature on the reaction rate was studied. The total  $\text{N}_2$  and  $\text{SO}_2$  flow rates in the experiments were controlled as 3450 mL/min, and the  $\text{SO}_2$  concentrations range from 3.0 to 9.0 v%, with an interval of 1.5 v%. The temperature effect on the reaction was studied in five different settings at intervals of 10°C, ranging from 20°C to 60°C.

### 2.4. Analysis of Lactic Acid with HPLC

The solutions obtained from the experiments were filtered with a 2.5  $\mu\text{m}$  filter paper to remove calcium sulfite particles. The filtered solutions were then analyzed using a Waters HPLC system, consisting of a Waters 501 HPLC pump and a Waters absorbance detector, to determine concentrations of lactic acid. The sample was passed through an Alltech Prevail

organic acid column (Alltech Associates, Inc.) with de-gassed  $\text{KH}_2\text{PO}_4$  (0.005 M) as the mobile phase and a flow rate of 0.8 mL/min, and was measured for lactic acid concentration using a detector with the UV light wavelength set at 192 nm.

### 3. Results and Discussion

When  $\text{SO}_2$  is sparged into a calcium lactate solution, a series of processes precede the reaction with the lactate anion solute in the solution. These processes include mass transfer at the gas-liquid interface and hydrolysis and ionization of the dissolved  $\text{SO}_2$ . The solubility of  $\text{SO}_2$  in 100 g of water is 10.6 g at a temperature of 20°C and 3.2 g at 60°C [7], indicating a potentially considerable buildup of dissolved  $\text{SO}_2$ . However, the rate at which  $\text{SO}_2$  was dissolved into water was so slow that differences of  $\text{SO}_2$  concentration in the inlet and outlet streams were negligible when there was only water in the reaction vessel. After adding calcium lactate to the water, the experiment indicated an  $\text{SO}_2$  concentration of nearly zero in the outlet stream during the first several minutes, suggesting that the solution's capacity for absorption of  $\text{SO}_2$  was greatly increased by the presence of calcium lactate [8]. When  $\text{SO}_2$  was introduced into the solution, it was dissolved into water and reacted with calcium lactate to produce calcium sulfite hemihydrate precipitate and lactic acid, since calcium sulfite has a much lower solubility than calcium lactate [9]. The lactic acid has a pKa of 3.86—much higher than the first-level pKa of sulfurous acid, 1.85 [7]. Correspondingly, the solid remaining in the solution after the reaction was mostly calcium sulfite, which can be separated from the liquid using a simple filtration process.

In the experimental design, the assumption was made that the reaction endpoint would be reached when concentrations of  $\text{SO}_2$  in the inlet and outlet mixture gases were identical. The

time needed for the completion of reaction between SO<sub>2</sub> and lactate is referred as reaction time. At the beginning of the reaction, SO<sub>2</sub> in the outlet gas from the reactor was nondetectable, indicating that the SO<sub>2</sub> in the gas mixture was completely removed by the reaction. With the progress of the reaction and consumption of calcium lactate, the remaining calcium lactate concentration in the reactor was not high enough to remove the introduced SO<sub>2</sub> instantly, thus leading to the increase of SO<sub>2</sub> concentration in the outlet gas. The time at which SO<sub>2</sub> began to appear in the outlet gas was referred to as the “breakthrough time.” At the end of the reaction, SO<sub>2</sub> was no longer consumed by or dissolved into the solution. Its concentration in the outlet gas was therefore the same as that in the inlet gas.

When 40.0 g of Ca(CH<sub>3</sub>CHOHCOO)<sub>2</sub> · 5H<sub>2</sub>O was added to 201.0 g of water, the amount that could be dissolved varied with temperature (i.e., 10.9 g at 20°C and 33.3 g at 50°C) [10]. The relationships among reaction temperature, reaction time, and the breakthrough time at given SO<sub>2</sub> concentrations are shown in Figures 1. Figure 1 indicates that the higher the reaction temperature, the shorter the reaction time needed, a phenomenon explained by kinetic theory (i.e., higher temperature results in a higher reaction rate constant). For example, reaction times at 60°C were only about 65 % of those at 20°C. Figure 1 also indicates that the breakthrough time decreased with the increase of the reaction temperature. The breakthrough times at 60°C were about 60 % of those at 20°C. In actual industrial application, these ratios would signify greater energy consumption in order to achieve a higher recovery rate at a fixed SO<sub>2</sub> flow rate.

Since the total gas flow rate was fixed, concentrations of SO<sub>2</sub> in the inlet stream under experimental conditions were proportional to its flow rate. Experimental results indicate that the concentration of SO<sub>2</sub> had a direct effect on the reaction time and breakthrough time: i.e.,

higher SO<sub>2</sub> concentrations led to decreases in both reaction time and breakthrough time at a given reaction temperature. Figure 1 shows that the reaction times needed at an SO<sub>2</sub> concentration of 9 v% were about 60% of those at the SO<sub>2</sub> concentration of 3 v%, while the breakthrough times at an SO<sub>2</sub> concentration of 9 v% were about 55 % of those at an SO<sub>2</sub> concentration of 3 v%. These results suggest that higher SO<sub>2</sub> concentrations were favorable to the reaction.

Results from the HPLC analyses (Table 1) show that SO<sub>2</sub> concentration and reaction temperature had no substantial effect on concentrations of produced lactic acid. Although there were some deviations from the designed 1.11 M of lactic acid concentration, these differences were random and did not indicate any effects from these two factors. Therefore, it is not necessary to control SO<sub>2</sub> concentrations and reaction temperatures within a specific range to make the process as a whole more efficient, which in turn suggests that SO<sub>2</sub> can be used to recover lactic acid from the calcium lactate solution at room temperature. Also, the ability of the calcium lactate solution to absorb SO<sub>2</sub> makes it a possible means of treating the flue gas from power plants [11, 12].

#### **4. Conclusions**

Sulfur dioxide can be used to recover lactic acid from calcium lactate solutions. The experimental results show that both the reaction time and breakthrough time decrease with the increase of reaction temperature and SO<sub>2</sub> concentration, respectively. Although a change of reaction conditions led to a change in reaction time, analysis of the produced lactic acid concentrations demonstrates that the complete conversion of calcium lactate to lactic acid was not affected. This suggests that the recovery process can be designed using a higher SO<sub>2</sub>

flow rate at room temperature without affecting recovery efficiency. Since energy for heating is substantially reduced, the latter feature is economically attractive for the industrial recovery of lactic acid from a biological fermentation broth. This paper's findings indicate that recovering lactic acid with SO<sub>2</sub> is both economical and environmentally beneficial.

### **Acknowledgement**

This research was funded by the U.S. Department of Agriculture. In addition, the authors wish to thank Ms. Desi Gunning of the Department of Biochemistry, Biophysics, and Molecular Biology at Iowa State University for her assistance in performing HPLC tests.

### **References**

- [1] C. H. Holten, A. Mueller, D. Rehbinder, Lactic acid properties and chemistry of lactic acid and derivatives, Verlag Chemie, Weinheim, Germany, 1971.
- [2] B. Urbas, Recovery of organic acids from a fermentation broth, U.S. Patent 4,444,881, 1984.
- [3] A. M. Baniel, A. M. Eyal, J. Mizrahi, B. Hazan, R. R. Fisher, J. J. Kolstad, B. F. Stewart, Lactic acid production, separation and/or recovery process, U.S. Patent 6,187,951, 2001.
- [4] N. A. Collins, M. R. Shelton, G. M. Tindall, S. T. Perri, R. S. O'Meadhra, C. W. Sink, B. K. Arumugam, J. C. Hubbs, Process for the recovery of organic acids from aqueous solutions, U.S. Patent 6,670,505, 2003.

- [5] A. D. Butler, M. Fan, R. C. Brown, A. T. Cooper, J. van Leeuwen, S. Sung, Absorption of dilute SO<sub>2</sub> gas stream with conversion to polymeric ferric sulfate for use in water treatment, *Chem. Eng. J.* 98 (3) (2004) 265-273.
- [6] M. Fan, R. C. Brown, Y. Zhuang, A. T. Cooper, M. Nomura, Reaction kinetics for a novel flue gas cleaning technology, *Environ. Sci. Technol.* 37 (7) (2003) 1404-1407.
- [7] D. R. Lide, *CRC handbook of chemistry and physics*, 84th ed., CRC Press, Boca Raton, Florida, 2003.
- [8] S. E. Schwartz, J. E. Freiberg, Mass-transport limitation to the rate of reaction of gases in liquid droplets: Application to oxidation of sulfur dioxide in aqueous solutions, *Atmos. Environ.* 15 (7) (1981) 1129-1144.
- [9] R. C. Weast, *CRC handbook of chemistry and physics*, 64th ed., CRC Press, Boca Raton, Florida, 1984.
- [10] S. K. Pateenko, V. A. Smirnov, Solubility of calcium lactate, *Khlebopek. Konditer. Prom.* 1 (1974) 27-29.
- [11] A. Durych, D. L. Wise, Y. A. Levendis, M. Metghalchi, *Industrial chemistry library*, Vol. 2: Calcium magnesium acetate. An emerging bulk chemical for environmental applications, Elsevier, Amsterdam, Netherlands, 1991.
- [12] H. Yoon, Flue gas desulfurization process, U.S. Patent 4,615,871, 1986.

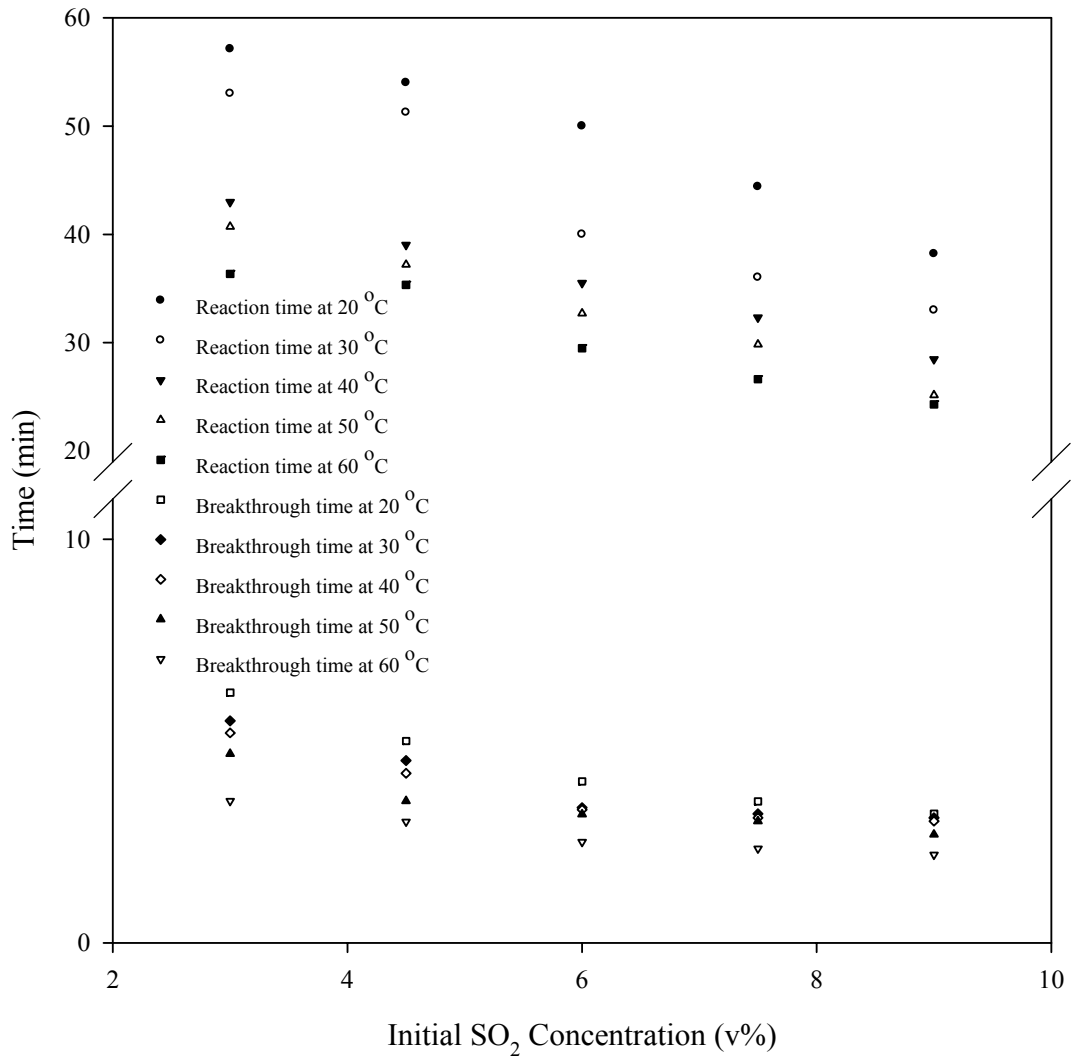


Fig. 1. The effect of SO<sub>2</sub> concentration and reaction temperature on breakthrough time and reaction time (flowrate of N<sub>2</sub> - SO<sub>2</sub> mixture: 3450 mL/min)



Table 1. Concentrations of produced lactic acid (M) under different experimental conditions

Temperature (°C)	20	30	40	50	60
SO <sub>2</sub> Concentration (v %)					
3.0	1.13 ± 0.04	1.09 ± 0.01	1.12 ± 0.05	1.11 ± 0.05	1.10 ± 0.03
4.5	1.10 ± 0.01	1.12 ± 0.02	1.10 ± 0.01	1.10 ± 0.00	1.10 ± 0.01
6.0	1.10 ± 0.04	1.09 ± 0.02	1.11 ± 0.02	1.11 ± 0.02	1.10 ± 0.02
7.5	1.13 ± 0.02	1.13 ± 0.02	1.13 ± 0.04	1.10 ± 0.00	1.11 ± 0.01
9.0	1.11 ± 0.05	1.13 ± 0.02	1.14 ± 0.01	1.10 ± 0.01	1.12 ± 0.01

## CHAPTER 4. CATALYTIC OXIDATION OF SULFUR DIOXIDE WITH MICROSCALE AND NANOSCALE IRON OXIDES AS CATALYSTS

A paper to be submitted to *Environmental Science and Technology*

Yonghui Shi<sup>1</sup>, Maohong Fan<sup>1,\*</sup>, Robert C. Brown<sup>1</sup>, J(Hans) van Leeuwen<sup>2</sup>, Chester Lo<sup>3</sup>,  
Guanghai Cao<sup>4</sup>, Ling Li<sup>1</sup> and Na Li<sup>1</sup>

<sup>1</sup>Center for Sustainable Environmental Technologies, Iowa State University, Ames, IA,  
50011, U. S. A.

<sup>2</sup>Department of Civil, Construction and Environmental Engineering, Iowa State University,  
Ames, IA, 50011, U.S.A.

<sup>3</sup>Center for Nondestructive Evaluation, Iowa State University, Ames, IA, 50011, U. S. A.

<sup>4</sup>Ames Lab, Iowa State University, Ames, 50011, U.S.A.

### **Abstract**

This paper contains a study of the oxidation of sulfur dioxide using microscale and nanoscale iron oxide as catalysts. A comparison of the catalytic performance of microscale and nanoscale iron oxides showed that nanoscale iron oxide is, in general, more effective than microscale iron oxide in catalyzing the oxidation of sulfur dioxide. The reaction orders with respect to the reactants sulfur dioxide and oxygen were determined when using microscale and nanoscale iron oxides as catalysts. Furthermore, the empirical Arrhenius expressions of

---

\*Corresponding author: e-mail: mfan@iastate.edu, phone: (515) 294-3951, fax: (515) 294-3091

catalytic oxidation of sulfur dioxide oxidation were derived based on the rate constants obtained at different temperatures.

## 1. Introduction

Sulfur dioxide ( $\text{SO}_2$ ) is the main source of acid rain and its emission is strictly restricted by the Clean Air Act (CAA) amendments of 1990.  $\text{SO}_2$  in the atmosphere originates from many sources, such as coal-fired power plants, petroleum refineries and diesel engines that use high sulfur fuel. Among all of the  $\text{SO}_2$  sources, the power plants contribute to more than 60 % of the pollution and are considered the major concern in EPA's  $\text{SO}_2$  reduction effort. Far more than a contributor of acid rain,  $\text{SO}_2$  is also associated with human respiratory disease. Those individuals, especially the elderly and children, and patients with heart or lung disease, are most vulnerable to the effect of  $\text{SO}_2$  pollution (1,2).

In spite of its negative effect on the environment and human health,  $\text{SO}_2$  is also an important raw material to produce a variety of chemicals in industries. **The power plants can now recover  $\text{SO}_2$  from flue gas and make it an economical feedstock to other industries (3,4).** Basically,  $\text{SO}_2$  can be converted to other chemicals through three routes: reduction, non-redox and oxidation reactions.  $\text{SO}_2$  is often reduced to sulfur by a modified Claus process, which has been widely used for sulfur recovery in petroleum refining or chemical industries (5). The non-redox  $\text{SO}_2$  utilization approaches are relatively simple and direct. For example,  $\text{SO}_2$  can be absorbed by sodium hydroxide or sodium carbonate to produce sodium sulfite. The oxidation of  $\text{SO}_2$  is the most frequently used method for its utilization. Many chemicals can be generated with the oxidation based approach. For example,  $\text{SO}_2$  can be oxidized to  $\text{SO}_3$  to produce fuming sulfuric acid through a contact process. Other oxidation based  $\text{SO}_2$

utilization includes the production of the sulfur-containing fertilizers, and sodium sulfate, an important chemical used in the manufacture of soap, paper and glass (6,7). Another oxidation based application was developed in our research group where SO<sub>2</sub> was used to synthesize polymeric ferric sulfate (8), a new coagulant for water and wastewater treatment (9-11).

The key step to oxidation based SO<sub>2</sub> utilization is expressed as:



Under the standard-state condition, i.e., 25 °C and 1 atm, the change in Gibbs free energy of the reaction,  $\Delta G^0$ , is -71 kJ/mol (12). Therefore, thermodynamically, the oxidation is feasible. However, the chemical kinetics of R1 limits its applicability. The oxidation is too slow at room temperature to be valuable for industry. In order to accelerate the rate of SO<sub>2</sub> oxidation, catalysts and high temperature are employed.

The currently used catalyst is vanadium pentoxide. There are two problems with the use of vanadium pentoxide. First, a high temperature is needed to achieve a high SO<sub>2</sub> conversion (13). Secondly, the application of vanadium pentoxide in industry raises a concern because research has shown that it is a pulmonary carcinogen (14,15). Precious metal catalysts can be used to avoid these problems, but they are very expensive and easily vitiated by certain impurities in SO<sub>2</sub>. A catalyst that is active at a low temperature, inexpensive, and environmentally friendly would be very desirable.

Iron oxide (Fe<sub>2</sub>O<sub>3</sub>) is an inexpensive alternative to the catalysts currently used. It occurs naturally as a mineral called hematite and is fairly active and selective for a number of heterogeneous catalytic reactions. Microscale Fe<sub>2</sub>O<sub>3</sub> has been successfully used as a catalyst for the oxidation of many air pollutants such as polychlorinated dibenzodioxin/dibenzofuran

(16) and SO<sub>2</sub> (17,18). Compared with microscale Fe<sub>2</sub>O<sub>3</sub>, nanoscale Fe<sub>2</sub>O<sub>3</sub> features with smaller particle size, higher specific surface area and greater concentration of catalytic active sites. These characteristics make nanoscale Fe<sub>2</sub>O<sub>3</sub> a more promising catalyst with significantly improved catalytic performance over its microscale counterpart. Unlike the expensive noble metal based catalysts, nanoscale Fe<sub>2</sub>O<sub>3</sub> catalyst is also expected to provide a more economical solution for modern industries. Recent studies have been made on the catalytic performance of nanoscale Fe<sub>2</sub>O<sub>3</sub> in many oxidation processes. For example, by using nanoscale Fe<sub>2</sub>O<sub>3</sub> as a catalyst, Li *et al.* reported that CO can be removed efficiently through catalytic oxidation (19). However, nanoscale Fe<sub>2</sub>O<sub>3</sub> has never been tested as a catalyst for the oxidation of SO<sub>2</sub>.

This paper focuses on deriving the chemical kinetics, reaction orders and Arrhenius expressions, of SO<sub>2</sub> oxidations using microscale and nanoscale Fe<sub>2</sub>O<sub>3</sub> as catalysts. The main objective of the research is to provide a basis for comparing microscale and nanoscale Fe<sub>2</sub>O<sub>3</sub> in catalyzing the oxidation of SO<sub>2</sub> in terms of economic and operational benefits.

## 2. Experimental Section

### 2.1. Materials

Microscale Fe<sub>2</sub>O<sub>3</sub> was procured from Bailey-PVS Oxides, LLC (Canonsburg, PA) and used as-received. BET surface analysis indicated that the microscale Fe<sub>2</sub>O<sub>3</sub> has a specific surface area of 4.0 m<sup>2</sup>/g. The nanoscale Fe<sub>2</sub>O<sub>3</sub> was purchased from Mach I Inc. (King of Prussia, PA). It is a brown superfine powder with a large specific surface area of 240.0 m<sup>2</sup>/g, which was specified by the manufacturer and confirmed by the BET surface analysis

conducted at Iowa State University. The physical properties and major chemical compositions of tested microscale and nanoscale iron oxides are shown in Table 1.

Pure O<sub>2</sub> and N<sub>2</sub>, certified SO<sub>2</sub> and O<sub>2</sub> were purchased from Linweld Inc. (Des Moines, IA) and used in the experiments. The certified SO<sub>2</sub> and O<sub>2</sub> had concentrations of 5000 ppm and 2500 ppm, respectively, and were balanced with N<sub>2</sub>.

### *2.2. Surface Area Measurement*

The surface area is an important factor affecting the activity and stability of a catalyst. The specific surface areas of the Fe<sub>2</sub>O<sub>3</sub> particles used in the experiments were measured with a Micromeritics® ASAP 2010 accelerated surface area and porosimetry system (Micromeritics, Norcross, GA).

### *2.3. Structure Characterization with Transmission Electron Microscopy*

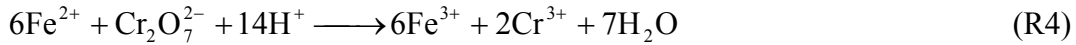
The structures of both microscale and nanoscale Fe<sub>2</sub>O<sub>3</sub> were characterized with transmission electron microscopy (TEM) bright field imaging and selected area electron diffraction (SAED) methods. The characterizations were carried out with a Philips CM30 electron microscope equipped with a LaB6 electron source, operated at an acceleration voltage of 300 kV.

### *2.4. Determination of Total Iron*

The total iron concentrations in the microscale and nanoscale Fe<sub>2</sub>O<sub>3</sub> powder were measured using a wet chemical method (20). According to this method, a specified amount of Fe<sub>2</sub>O<sub>3</sub> powder was dissolved using hydrochloric acid. The solution was then treated with

stannous chloride and titanous trichloride sequentially to reduce  $Fe^{3+}$  to  $Fe^{2+}$ . The concentration of  $Fe^{2+}$  in iron chloride solution was titrated with a standard potassium dichromate solution.

The chemical reactions involved in this method are shown as follows:



The total iron concentration  $C_{Fe}$  (wt%) in iron chloride solution was expressed as:

$$C_{Fe} = \frac{V \times C \times 0.5585 \times 6}{m} \times 100 \quad (1)$$

where  $V$  is the volume (mL) of potassium dichromate standard solution consumed at the titration end point,  $C$  is the concentration (M) of the standard potassium dichromate solution,  $m$  is the mass (g) of the iron chloride solution sample, and 0.05585 is the mass (g) of 0.001 mole of elemental iron.

The total iron concentration (wt%) in  $Fe_2O_3$  powder is expressed as

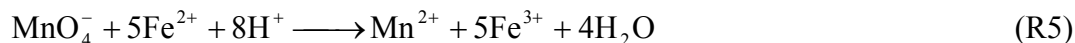
$$X_{Fe} = \frac{C_{Fe} \times m_{Fe}}{m_{Fe_2O_3}} \quad (2)$$

where  $X_{Fe}$  is the total iron concentration (wt%) in the microscale or nanoscale  $Fe_2O_3$  powder,  $m_{Fe}$  is the mass of the iron chloride solution and  $m_{Fe_2O_3}$  is the mass (g) of the microscale or nanoscale  $Fe_2O_3$ .

### 2.5. Determination of $Fe^{2+}$ and $Fe^{3+}$

A specified amount of microscale or nanoscale  $Fe_2O_3$  powder was dissolved using

hydrochloric acid to make iron chloride solution. The solution was treated with sulfuric acid and phosphoric acid followed by the titration of  $\text{Fe}^{2+}$  using a standard potassium permanganate solution (20). The principle of this method is shown as follows



The ferrous iron concentration  $C_{\text{Fe}^{2+}}$  (wt%) in the iron chloride solution can be calculated as:

$$C_{\text{Fe}^{2+}} = \frac{(V - V_0) \times C \times 0.5585}{m} \times 100 \times 5 \quad (3)$$

where  $V$  is the volume (mL) of the potassium permanganate consumed by the iron chloride solution at the titration end point,  $V_0$  is the volume (mL) of the standard potassium permanganate solution consumed by a blank distilled water at the titration end point,  $C$  is the concentration (M) of the standard potassium permanganate solution,  $m$  is the mass (g) of the iron chloride solution sample, and 0.5585 is the mass (g) of 0.001 mole of elemental iron.

The  $\text{Fe}^{2+}$  concentration (wt%) in  $\text{Fe}_2\text{O}_3$  powder is expressed as

$$X_{\text{Fe}^{2+}} = \frac{C_{\text{Fe}^{2+}} \times m_{\text{Fe}}}{m_{\text{Fe}_2\text{O}_3}} \quad (4)$$

where  $X_{\text{Fe}^{2+}}$  is  $\text{Fe}^{2+}$  concentration (wt%) in microscale or nanoscale  $\text{Fe}_2\text{O}_3$ ,  $m_{\text{Fe}}$  is the mass of the iron chloride solution,  $m_{\text{Fe}_2\text{O}_3}$  is the mass (g) of the microscale or nanoscale  $\text{Fe}_2\text{O}_3$ .

Therefore, the  $\text{Fe}^{3+}$  concentration (wt%) in  $\text{Fe}_2\text{O}_3$  powder is expressed as

$$X_{\text{Fe}^{3+}} = X_{\text{Fe}} - X_{\text{Fe}^{2+}} \quad (5)$$

where  $X_{\text{Fe}^{3+}}$  is  $\text{Fe}^{3+}$  concentration (wt%) in the microscale or nanoscale  $\text{Fe}_2\text{O}_3$ .

**2.6. Apparatus and Operation Procedures.** The laboratory set-up used for the research



is shown in Figure 1. The SO<sub>2</sub> oxidation experiments were carried out using a quartz tube reactor. In the middle of the quartz tube, Fe<sub>2</sub>O<sub>3</sub> catalyst powder was located with quartz wool on both sides to avoid catalyst loss caused by gas flow. The quartz tube with catalyst was then placed inside a TF55030A-1 tube furnace from Lindberg/Blue M (Asheville, NC). The temperature of the tube furnace was controlled with a UT150 temperature controller (Yokogawa M&C Corporation, Newnan, GA). The flows of the SO<sub>2</sub>, O<sub>2</sub> and N<sub>2</sub> were controlled with a C-03217-52 150 mm Teflon correlated flowmeter (Cole Parmer, Vernon Hills, IL), a C-03229-11 150 mm correlated flowmeter (Cole Parmer) and a Gilmont Instrument 150 mm direct reading flowmeter (Cole Parmer), respectively. The flowmeters were calibrated with a bubble meter before the experiments. The total flow rate of the mixture gas, 50 mL/min, was used for all the tests.

Before entering the quartz tube, SO<sub>2</sub>, O<sub>2</sub> and N<sub>2</sub> were mixed to produce a gas mixture with predetermined concentrations of SO<sub>2</sub> and O<sub>2</sub>. The gas mixture was balanced with nitrogen in each test. In order to remove water vapor and particles that may be present in the system, the effluent gas from the quartz tube first passed a Permapure model MD-110-48F-2 Nafion concentric tube dryer (Permapure, Toms River, NJ) and then through a Cole Parmer 0.2 micron in-line particulate filter. Finally, the concentration of SO<sub>2</sub> after the reaction in the effluent gas stream was measured with a California Analytical model ZRF NDIR gas analyzer. The analyzer was connected to a computer system that recorded the SO<sub>2</sub> concentrations, which were used for calculating the oxidation efficiencies of SO<sub>2</sub>.

A continuous packed bed catalytic reactor was used in all the SO<sub>2</sub> oxidation tests in this study. The degree to which the volumetric flow rate of gas stream before and after oxidation is changed, should be evaluated in order to determine whether the changes have significant

effects on the accuracies of kinetic model derivations. Assume the flow rate (mol/s) of gas mixture fed into the reactor is  $F$ , the molar ratio of  $\text{SO}_2$ ,  $\text{O}_2$  and  $\text{N}_2$  in the feeding gas mixture is  $y_{\text{SO}_2,0}$ ,  $y_{\text{O}_2,0}$  and  $y_{\text{N}_2,0}$ , respectively, and the conversion of  $\text{SO}_2$  to  $\text{SO}_3$  is  $X$ , then the effluent stream consists of  $\text{SO}_2$ ,  $\text{O}_2$ ,  $\text{SO}_3$  and  $\text{N}_2$ , with the flow rates (mol/s) as  $y_{\text{SO}_2,0}F(1-X)$ ,  $(y_{\text{O}_2,0} - \frac{1}{2}Xy_{\text{SO}_2,0})F$ ,  $Xy_{\text{SO}_2,0}F$  and  $y_{\text{N}_2,0}F$ , respectively. Therefore, the flow rate (mol/s) of gas mixture leaving the reactor can be expressed as

$$n_{\text{Total}} = (1 - \frac{1}{2}X \cdot y_{\text{SO}_2,0})F \quad (6)$$

The maximum  $\text{SO}_2$  concentration used in the whole research was 2000 ppm, which resulted in only 0.1 % change in the volume of gas mixture. Therefore, the change in volume of gas mixture before and after reaction can be considered to be negligible.

Baseline tests were conducted under different temperatures to check whether oxidation of  $\text{SO}_2$  occurred without the presence of catalysts. The tested temperature range is 500~1000 °C with an interval of 50 °C.

The flow rates of 30, 40, 50, 60 and 70 mL/min were used to study the effects of total flow rate on the  $\text{SO}_2$  conversion under the temperatures of 470 °C and 330 °C for microscale and nanoscale  $\text{Fe}_2\text{O}_3$  respectively. The concentration of  $\text{SO}_2$  used in this particular study was 1200 ppm.

To derive the reaction order for  $\text{SO}_2$ , experiments were arranged with  $\text{SO}_2$  concentrations of 400 ppm, 800 ppm, 1200 ppm, 1600 ppm and 2000 ppm while the initial concentration of  $\text{O}_2$  was 50 v%. In all the experiments for calculating  $\text{SO}_2$  reaction order, the concentrations of  $\text{O}_2$  in the gas mixture were at least 250 times the stoichiometric amount of  $\text{O}_2$  needed for

complete oxidation of  $\text{SO}_2$ . To establish the reaction order with respect to  $\text{O}_2$  the initial concentrations of  $\text{O}_2$  used ranged from 200 to 1000 ppm with an interval of 200 ppm and the initial concentrations of  $\text{SO}_2$  were always twice that of  $\text{O}_2$ . The microscale and nanoscale  $\text{Fe}_2\text{O}_3$  based catalytic oxidation tests used for obtaining the reaction order for  $\text{SO}_2$  were undertaken at 500 °C and 320 °C, respectively. The temperatures selected for conducting tests for calculating the reaction order for  $\text{O}_2$  were 650 °C and 400°C with respect to microscale and nanoscale  $\text{Fe}_2\text{O}_3$ , respectively.

### 3. Results and Discussion

#### 3.1. Structure of Microscale and Nanoscale $\text{Fe}_2\text{O}_3$

According to Figures 2a and 3a, the bright-field TEM images showed that the size of microscale  $\text{Fe}_2\text{O}_3$  is in the range of 100~200 nm, while that of the nanoscale  $\text{Fe}_2\text{O}_3$  is only about 3 nm. The selected area electron diffraction (SAED) pattern in Figure 2b of one of the microscale  $\text{Fe}_2\text{O}_3$  particles along the [001] zone axis, showed that  $\text{Fe}_2\text{O}_3$  has a hexagonal structure with the lattice parameters  $a$  and  $c$  as 5.0 Å and 13.6 Å respectively. The SAED pattern of nanoscale  $\text{Fe}_2\text{O}_3$  in Figure 3b indicated that the  $\text{Fe}_2\text{O}_3$  particle is in the form of polycrystalline, which also has a hexagonal structure.

#### 3.2. Baseline

The results of tests on the non-catalytic oxidation of  $\text{SO}_2$  are presented in the Figure 4. Figure 4 shows that  $\text{SO}_2$  can not be oxidized at all by  $\text{O}_2$  without help of a catalyst even at a temperature of 1000 °C. Therefore, catalysts are necessary for the oxidation of  $\text{SO}_2$  to occur in an economically feasible temperature range.

### 3.3. Effects of Temperatures

The changes in the SO<sub>2</sub> conversion to SO<sub>3</sub> in the presence of microscale and nanoscale Fe<sub>2</sub>O<sub>3</sub> in the temperature range of 100~1000 °C are depicted in Figure 4. These results indicated that microscale and nanoscale Fe<sub>2</sub>O<sub>3</sub> catalysts can substantially enhance the oxidation of SO<sub>2</sub>. Furthermore, four more facts are shown in Figure 4. Firstly, it indicated that SO<sub>2</sub> conversion catalyzed by microscale or nanoscale Fe<sub>2</sub>O<sub>3</sub> was a function of temperature. Secondly, the onset reaction temperature of SO<sub>2</sub> oxidation for nano Fe<sub>2</sub>O<sub>3</sub> was about 150 °C while that for microscale Fe<sub>2</sub>O<sub>3</sub> was 200 °C. The difference in onset temperature may be explained by the fact that the nano Fe<sub>2</sub>O<sub>3</sub> is typically better than microscale Fe<sub>2</sub>O<sub>3</sub> in lowering activation energy of oxidations of chemicals (19). Thirdly, SO<sub>2</sub> can be almost completely oxidized when nanoscale Fe<sub>2</sub>O<sub>3</sub> was used as a catalyst at 450 °C while the maximum conversion of SO<sub>2</sub> was only 84% under the catalysis of microscale Fe<sub>2</sub>O<sub>3</sub> even at 650 °C. Fourthly, the SO<sub>2</sub> conversion catalyzed by both Fe<sub>2</sub>O<sub>3</sub> decreased with the increase of temperature above 650 °C and 500 °C for microscale and nanoscale Fe<sub>2</sub>O<sub>3</sub>, respectively. Therefore, nanoscale Fe<sub>2</sub>O<sub>3</sub> was more effective than microscale Fe<sub>2</sub>O<sub>3</sub> in catalyzing the oxidation of SO<sub>2</sub>.

### 3.4. Reaction Orders for SO<sub>2</sub> and Oxygen

Assuming that  $C_{SO_2,0}$ ,  $C_{O_2,0}$  and  $C_{SO_3,0}$  are the initial concentrations (M) of reactants SO<sub>2</sub>, O<sub>2</sub> and SO<sub>3</sub>, and  $C_{SO_2}$ ,  $C_{O_2}$  and  $C_{SO_3}$  represent the concentrations (M) of SO<sub>2</sub>, O<sub>2</sub> and SO<sub>3</sub> in the effluent stream when the reaction is in steady state, respectively, then the SO<sub>2</sub> concentration difference between influent and effluent in the steady state can be expressed as

$C_{SO_2,0} - C_{SO_2}$ . Based on the stoichiometric relationship between  $SO_2$  and  $O_2$  shown as R1, the consumed  $O_2$  and produced  $SO_3$  at the steady state can be expressed as  $0.5(C_{SO_2,0} - C_{SO_2})$  and  $C_{SO_2,0} - C_{SO_2}$ . Assuming that the volumetric flow rate of gas mixture is  $v_0$  (L/s), then the rates of  $SO_2$ ,  $O_2$  consumption and  $SO_3$  generation,  $\Delta F_{SO_2}$ ,  $\Delta F_{O_2}$  and  $\Delta F_{SO_3}$  (mol/s), can be expressed as follows

$$\Delta F_{SO_2} = v_0 (C_{SO_2,0} - C_{SO_2}) \quad (7)$$

$$\Delta F_{O_2} = 0.5v_0 (C_{SO_2,0} - C_{SO_2}) \quad (8)$$

$$\Delta F_{SO_3} = v_0 (C_{SO_2,0} - C_{SO_2}) \quad (9)$$

The reaction rate of the catalytic  $SO_2$  oxidation (R1) in terms of  $SO_2$  can be expressed as

$$-r_{SO_2} = \frac{dF_{SO_2}}{dW} \quad (10)$$

For a differential reactor, the reaction rate can be expressed as

$$-r_{SO_2} = \frac{dF_{SO_2}}{dW} = \frac{\Delta F_{SO_2}}{\Delta W} \quad (11)$$

where  $\Delta W$  is the mass (g) of catalyst loaded. Similarly, the reaction rates (mol/g's) of R1,  $r_{O_2}$  and  $r_{SO_3}$ , in term of  $O_2$  and  $SO_3$ , can be expressed respectively as follows

$$r_{O_2} = -\frac{\Delta F_{O_2}}{\Delta W} \quad (12)$$

and

$$r_{SO_3} = \frac{\Delta F_{SO_3}}{\Delta W} \quad (13)$$

It is obvious that the following relationships among  $r_{SO_2}$ ,  $r_{O_2}$  and  $r_{SO_3}$  exist:

$$-r_{SO_2} = -2r_{O_2} = r_{SO_3} \quad (14)$$

In all the tests, the inlet and outlet concentrations of SO<sub>2</sub> in gas streams were measured. The reaction rate in term of SO<sub>2</sub>,  $r_{SO_2}$ , was used to calculate the rate constant and reaction orders of R1 using the following relationship:

$$-r_{SO_2} = \frac{v_0(C_{SO_2,0} - C_{SO_2})}{\Delta W} = kC_{SO_2}^{\alpha_{SO_2}} C_{O_2}^{\alpha_{O_2}} \quad (15)$$

where  $k$  represents the reaction rate constant and exponents  $\alpha_{SO_2}$  and  $\alpha_{O_2}$  are the reaction orders with respect to reactants SO<sub>2</sub> and O<sub>2</sub>. Reaction orders  $\alpha_{SO_2}$  and  $\alpha_{O_2}$  are not necessarily integers because R1 is not an elementary reaction.

Special initial reactant concentrations were chosen in order to derive reaction orders  $\alpha_{SO_2}$  and  $\alpha_{O_2}$ . When  $\alpha_{SO_2}$  was to be established,  $C_{O_2,0}$  was designed to be much larger than  $C_{SO_2,0}$  and so that  $C_{O_2}$  at any time of the reaction can be considered as a constant. Then the reaction rate of R1, with respect to SO<sub>2</sub>, can be expressed as:

$$\frac{v_0(C_{SO_2,0} - C_{SO_2})}{\Delta W} = k' C_{SO_2}^{\alpha_{SO_2}} \quad (16)$$

where  $k' = kC_{O_2}^{\alpha_{O_2}}$ . Taking the logarithm of Eq. 16 yields Eq.17

$$\ln\left(\frac{v_0(C_{SO_2,0} - C_{SO_2})}{\Delta W}\right) = \ln k' + \alpha_{SO_2} \ln C_{SO_2} \quad (17)$$

Based on Eq. 17, a series of tests were designed at a specified temperature  $T$ , where the initial concentrations of SO<sub>2</sub> were varied and the initial concentrations of O<sub>2</sub> were set at a level much higher than those of SO<sub>2</sub>. For each test under a given initial SO<sub>2</sub> concentration ( $C_{SO_2,0}$ ),

two sets of data  $\left( \ln \left( \frac{v_0 (C_{SO_2,0} - C_{SO_2})}{\Delta W} \right), C_{SO_2} \right)$  were collected. Based on the data obtained from different initial SO<sub>2</sub> concentration ( $C_{SO_2,0}$ ), a graph of  $\ln \left( \frac{v_0 (C_{SO_2,0} - C_{SO_2})}{\Delta W} \right)$  versus  $\ln C_{SO_2}$  can be plotted to calculate  $\alpha_{SO_2}$ .

Due to the limit of the concentration measurement range (0~10 v%) of the SO<sub>2</sub> analyzer used in the project, the reaction order  $\alpha_{O_2}$  cannot be established with the same method as aforementioned. To derive the reaction order  $\alpha_{O_2}$ , reactions were designed in such a way where the initial concentrations of SO<sub>2</sub> were always two times of those of O<sub>2</sub> at any temperature  $T$ . Consequently, at any time of the reaction, the concentrations of SO<sub>2</sub> and O<sub>2</sub> in the effluent have a relationship shown as follows

$$C_{SO_2} = 2C_{O_2} \quad (18)$$

Then the reaction rate with respect to SO<sub>2</sub> can be expressed as

$$-r_{SO_2} = \frac{v_0 (C_{SO_2,0} - C_{SO_2})}{\Delta W} = k C_{SO_2}^{\alpha_{SO_2}} \left( \frac{C_{SO_2}}{2} \right)^{\alpha_{O_2}} = \frac{k}{2^{\alpha_{O_2}}} C_{SO_2}^{\alpha_{SO_2} + \alpha_{O_2}} \quad (19)$$

Taking the logarithm of Eq. 19 yields Eq. 20.

$$\ln(-r_{SO_2}) = \ln k - \alpha_{SO_2} \ln 2 + (\alpha_{SO_2} + \alpha_{O_2}) \ln C_{SO_2} \quad (20)$$

Based on Eq. 20 and  $\alpha_{SO_2}$  obtained from Eq. 17, the reaction order,  $\alpha_{O_2}$ , along with the reaction rate constant,  $k$ , at a given temperature  $T$ , can be derived.

According to Eq. 17, the reaction orders for SO<sub>2</sub> for the microscale and nanoscale Fe<sub>2</sub>O<sub>3</sub> catalysts ( $\alpha_{SO_2, Micro}$  and  $\alpha_{SO_2, Nano}$ ) are shown as the slopes of the lines in Figure 5 and 6, respectively. From these two figures, it can be seen that the reactions are both first order for

SO<sub>2</sub> no matter which type of Fe<sub>2</sub>O<sub>3</sub> catalyst was used. The reaction orders in respect of O<sub>2</sub> for the microscale and nanoscale Fe<sub>2</sub>O<sub>3</sub> catalysts ( $\alpha_{O_2, Micro}$  and  $\alpha_{O_2, Nano}$ ) are shown in Figure 7 and Figure 8, respectively. According to Figure 7, Eq. 20 is written as Eq. 21.

$$\ln(-r_{SO_2}) = -4.84 + 1.24 \ln C_{SO_2} \quad (21)$$

The equation set, Eq. 22 and 23, can be obtained as follows from Eq. 21.

$$\alpha_{SO_2, Micro} + \alpha_{O_2, Micro} = 1.24 \quad (22)$$

$$\ln k - \alpha_{O_2, Micro} \ln 2 = -4.84 \quad (23)$$

Therefore, the reaction order with respect to O<sub>2</sub> for the microscale Fe<sub>2</sub>O<sub>3</sub> as catalyst,  $\alpha_{O_2, Micro}$ , is 0.24, and the natural logarithm of the reaction rate constant at the temperature of 650 °C is -4.67.

Using the same method, the reaction order for the nanoscale Fe<sub>2</sub>O<sub>3</sub> as catalyst,  $\alpha_{O_2, Nano}$ , is 0.30, and the natural logarithm of the reaction rate constant at the temperature of 400 °C as -2.19. Consequently, the rate of SO<sub>2</sub> consumption for the microscale and nanoscale Fe<sub>2</sub>O<sub>3</sub> as catalysts ( $-r_{SO_2, Micro}$  and  $-r_{SO_2, Nano}$ ) can be expressed as

$$-r_{SO_2, Micro} = k_{Micro} C_{SO_2} C_{O_2}^{0.24} \quad (24)$$

$$-r_{SO_2, Nano} = k_{Nano} C_{SO_2} C_{O_2}^{0.30} \quad (25)$$

where  $k_{Micro}$  and  $k_{Nano}$  stand for reaction rate constants when microscale and nanoscale Fe<sub>2</sub>O<sub>3</sub> are used as catalysts respectively.



### 3.5. Reaction Constant $k$ and Apparent Activation Energy $E_a$

The relationship between reaction rate constant,  $k$ , and reaction temperature,  $T$ , can be expressed in the empirical Arrhenius equation

$$k = Ae^{-\frac{E_a}{RT}} \quad (26)$$

where  $A$  is the pre-exponential factor,  $E_a$  is the apparent activation energy of the reaction, and  $R$  is the ideal gas constant. When the relationships of  $\ln k$  versus  $1/T$  are plotted,  $E_a$  and  $A$  in Eq. 26 can be derived with the slope  $-E_a/R$  and interception  $\log A$  of the plot, respectively.

The Arrhenius relationship was determined by changing the reaction temperature with the reactant concentrations kept unchanged. For the reaction with the use of microscale  $\text{Fe}_2\text{O}_3$  as catalyst, the temperature range was 450 to 650 °C, with an interval of 50 °C. For the experiments that used nanoscale  $\text{Fe}_2\text{O}_3$  catalyst, the temperature range was 300 to 500 °C, with an interval of 50 °C.

Fixing the input  $\text{SO}_2$  and  $\text{O}_2$  concentrations as 1600 and 800 ppm respectively, a series of reaction rates,  $-r_{\text{SO}_2}$ , can be obtained according to Eq. 15 at different temperatures.

Consequently, the reaction rate constants,  $k$ , at different temperatures can be calculated with Eq. 20. When the microscale  $\text{Fe}_2\text{O}_3$  is used as catalyst, the reaction temperature and reaction rate constant are shown in Table 2, and the relationship between  $\ln k$  and  $1/T$  is plotted in Figure 9. From Figure 9 and Eq. 26, the apparent activation energy  $E_{a\text{Micro}}$  and pre-exponential factor  $A_{\text{Micro}}$  for microscale  $\text{Fe}_2\text{O}_3$  were calculated to be 32.8 kJ/mol and 0.7, respectively. In the case of nanoscale  $\text{Fe}_2\text{O}_3$  catalyst, the reaction temperature, reaction constant rate are shown in Table 3 and the relationship between  $\ln k$  and  $1/T$  is plotted in

Figure 10. The apparent activation energy  $E_{a\ Nano}$  and pre-exponential factor  $A_{Nano}$  for nanoscale  $Fe_2O_3$  are 17.4 kJ/mol and 2.6, respectively.

The Arrhenius equation for the microscale and nanoscale  $Fe_2O_3$  catalysts, can be written as

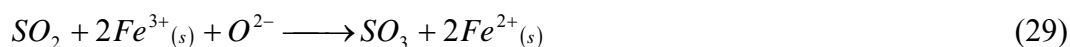
$$k_{Micro} = 0.7e^{-\frac{3944}{T}} \left( \text{mol}^{-0.24} \cdot \text{dm}^{3.72} \cdot \text{s}^{-1} \cdot \text{g}^{-1} \right) \quad (27)$$

$$k_{Nano} = 2.6e^{-\frac{2099}{T}} \left( \text{mol}^{-0.30} \cdot \text{dm}^{3.90} \cdot \text{s}^{-1} \cdot \text{g}^{-1} \right) \quad (28)$$

It can be seen that the apparent activation energy of the reaction decreased by about 50 % when using nanoscale  $Fe_2O_3$  as catalyst in comparison with the case using microscale  $Fe_2O_3$ . Activation energy is a direct indication of whether a reaction is easy to happen. This explains the experimental results found in this study that the reaction is liable to take place at lower temperatures (less than 200 °C) when nanoscale  $Fe_2O_3$  was used as catalyst. The improvement in the  $SO_2$  conversion by using nanoscale  $Fe_2O_3$  may also be demonstrated by its tendency to decrease the activation energy of the reaction. Nanoscale  $Fe_2O_3$  was shown, in a previous CO oxidation study, to be effective in decreasing the activation energy from 20 kcal/mol, the value for using microscale  $Fe_2O_3$ , to 14.5 kcal/mol (19). It was reported that the adsorption of  $SO_2$  on  $Fe_2O_3$  controlled the reaction rate (21), which means that a high specific surface area will be favorable to the reaction. Due to its high surface area, and correspondingly the potential to lower activation energy, nanoscale  $Fe_2O_3$ , therefore, is more effective than microscale  $Fe_2O_3$  as a catalyst to remove  $SO_2$  from flue gas.

### 3.6. The Reaction Mechanism of SO<sub>2</sub> Catalytic Oxidation

The reaction orders derived from the experiments indicated that the oxidation of SO<sub>2</sub> is nonelementary, which means that the reaction mechanism is rather complex and may consist of several steps. Similarly, SO<sub>2</sub> oxidation catalyzed by the commercial vanadium pentoxide is also suggested to have a complex mechanism. Although the SO<sub>2</sub> oxidation using vanadium pentoxide as a catalyst has a long history, the mechanism behind the apparently simple reaction is still under debate (22). A wide range of apparent activation energy values for the reaction catalyzed by vanadium pentoxide were reported by many researchers (23,24), all of the values higher than those for the reactions catalyzed by Fe<sub>2</sub>O<sub>3</sub>. In industry practice, a conversion of as high as 99 % can be obtained by using vanadium pentoxide at a temperature around 450 °C (22). In view of this fact, microscale Fe<sub>2</sub>O<sub>3</sub> will not be considered as an alternative, whereas nanoscale Fe<sub>2</sub>O<sub>3</sub> may serve as a potential replacement since it brings about a competitive SO<sub>2</sub> conversion with similar reaction temperature. The possible reaction mechanism for SO<sub>2</sub> oxidation catalyzed by Fe<sub>2</sub>O<sub>3</sub> is proposed as follows:



It can be concluded that the oxidation of SO<sub>2</sub> was facilitated with both microscale and nanoscale Fe<sub>2</sub>O<sub>3</sub> powders serving as catalysts. The performance of nanoscale Fe<sub>2</sub>O<sub>3</sub> was found to be superior to its microscale counterpart. Compared with microscale Fe<sub>2</sub>O<sub>3</sub>, nanoscale Fe<sub>2</sub>O<sub>3</sub> not only substantially decreases the onset reaction temperature, but also increases the SO<sub>2</sub> conversion efficiency. The apparent activation energies and reaction orders for SO<sub>2</sub> and O<sub>2</sub> were obtained with the kinetic models established for the SO<sub>2</sub> oxidation

reaction catalyzed by both types of  $\text{Fe}_2\text{O}_3$ . The apparent activation energy of the reaction catalyzed by nanoscale  $\text{Fe}_2\text{O}_3$  was only half of that for the reaction catalyzed by microscale  $\text{Fe}_2\text{O}_3$ . The comparison between  $\text{Fe}_2\text{O}_3$  and commercial vanadium pentoxide suggested that nanoscale  $\text{Fe}_2\text{O}_3$  performed competitively with vanadium pentoxide in catalyzing  $\text{SO}_2$  oxidation and had a potential to be used as an alternative catalyst.

### References

- (1) Jaeger, M. J.; Tribble, D.; Wittig, H. J. Effect of 0.5 ppm sulfur dioxide on the respiratory function of normal and asthmatic subjects. *Lung* **1979**, *156*, 119-27.
- (2) Witek, T. J.; Schachter, E. N.; Beck, G. J.; Cain, W. S.; Colice, G.; Leaderer, B. P. Respiratory symptoms associated with sulfur dioxide exposure. *Int. Arch. Occup. Environ. Health* **1985**, *55*, 179-83.
- (3) Kikkinides, E. S.; Yang, R. T. Simultaneous sulfur dioxide/nitrogen oxide ( $\text{NO}_x$ ) removal and sulfur dioxide recovery from flue gas by pressure swing adsorption. *Ind. Eng. Chem. Res.* **1991**, *30* (8), 1981-1989.
- (4) Williams, N.; Srinivasan, G., Wechselblatt, P. Removal and recovery of  $\text{SO}_2$  from power station flue gases. *Chem. Ingen. Techn.* **1973**, *45* (7), 437-441.
- (5) Davydov, A. A.; Marshneva, V. I.; Shepotko, M. L. Metal oxides in hydrogen sulfide oxidation by oxygen and sulfur dioxide I. The comparison study of the catalytic activity. Mechanism of the interactions between  $\text{H}_2\text{S}$  and  $\text{SO}_2$  on some oxides. *Appl. Catal. A: Gen.* **2003**, *244*, 93-100.

- (6) Stankowski, S.; Murkowski, A.; Malinowski, R. Possibilities of utilization of a byproduct from removing SO<sub>2</sub> and NO<sub>x</sub> from flue gases as a nitrogen-sulfur fertilizer. *Folia Univ. Agric. Stetin.* **1998**, *190*, 277-281.
- (7) Satrio, J. A. B.; Jagtap, S. B.; Wheelock, T. D. Utilization of sulfur oxides for the production of sodium sulfate. *Ind. Eng. Chem. Res.* **2002**, *41*, 3540-3547.
- (8) Fan, M.; Sung, S.; Brown, R. C.; Wheelock, T. D.; Laabs, F. C. Synthesis, characterization, and coagulation of polymeric ferric sulfate. *J. Environ. Eng.* **2002**, *128*, 483-490.
- (9) Fan, M.; Brown, R. C.; Zhuang, Y.; Cooper, A. T.; Nomura, M. Reaction kinetics for a novel flue gas cleaning technology. *Environ. Sci. Technol.* **2003**, *37*, 1404-1407.
- (10) Butler, A. D.; Fan, M.; Brown, R. C.; Cooper, A. T.; van Leeuwen, J. (H); Sung, S. Absorption of dilute SO<sub>2</sub> gas stream with conversion to polymeric ferric sulfate for use in water treatment. *Chem. Eng. J.* **2004**, *98*, 265-273.
- (11) Butler, A. D.; Fan, M.; Brown, R. C.; van Leeuwen, J.; Sung, S.; Duff, B. Pilot-scale tests of poly ferric sulfate synthesized using SO<sub>2</sub> at Des Moines Water Works. *Chem. Eng. Proc.* **2004**, *44*, 413-419.
- (12) *CRC Handbook of Chemistry and Physics*, 84th ed.; Lide, D. R., Ed.; CRC Press: Boca Raton, FL, 2003.

- (13) Dunn, J. P.; Stenger, H. G.; Wachs, I. E. Molecular structure-reactivity relationships for the oxidation of sulfur dioxide over supported metal oxide catalysts. *Catal. Today* **1999**, *53*, 543-556.
- (14) Ress, N. B.; Chou, B. J.; Renne, R. A.; Dill, J. A.; Miller, R. A.; Roycroft, J. H.; Hailey, J. R.; Haseman, J. K.; Bucher, J. R. Carcinogenicity of inhaled vanadium pentoxide in F344/N rats and B6C3F1 mice. *Toxicol. Sci.* **2003**, *74*, 287-296.
- (15) Zhang, L.; Rice, A. B.; Adler, K.; Sannes, P.; Martin, L.; Gladwell, W.; Koo, J. S.; Gray, T. E.; Bonner, J. C. Vanadium stimulates human bronchial epithelial cells to produce heparin-binding epidermal growth factor-like growth factor: a mitogen for lung fibroblasts. *Am. J. Respir. Cell Mol. Biol.* **2001**, *24*, 123-131.
- (16) Lomnicki, S.; Dellinger, B. Development of supported iron oxide catalyst for destruction of PCDD/F. *Environ. Sci. Technol.* **2003**, *37*, 4254-4260.
- (17) Tseng, H. H.; Wey, M. Y.; Liang, Y. S.; Chen, K. H. Catalytic removal of SO<sub>2</sub>, NO and HCl from incineration flue gas over activated carbon-supported metal oxides. *Carbon* **2003**, *41*, 1079-1085.
- (18) Ma, J.; Liu, Z.; Liu, S.; Zhu, Z. A regenerable Fe/AC desulfurizer for SO<sub>2</sub> adsorption at low temperatures. *Appl. Catal. B Environ.* **2003**, *45*, 301-309.
- (19) Li, P.; Miser, D. E.; Rabiei, S.; Yadav, R. T.; Hajaligol, M. R. The removal of carbon monoxide by iron oxide nanoparticles. *Appl. Catal. B Environ.* **2003**, *43*, 151-162.

- (20) *Peking University's analytical chemistry experiment manual*; Beijing University: Beijing, 1993.
- (21) Chung, K. C.; Quon, J. E. Capacity of ferric oxide particles to oxidize sulfur dioxide in air. *Environ. Sci. Technol.* **1973**, 7, 532-8.
- (22) Kenney, C. N. The catalytic oxidation of sulfur dioxide. *Catalysis* **1980**, 3, 123-35.
- (23) Simecek, A.; Kadlec, B.; Michalek, J. Reduction-oxidation mechanism of sulfur dioxide oxidation on vanadium catalysts. *J. Catal.* **1969**, 14 (4), 287-292.
- (24) Calderbank, P. H. Contact-process converter design. *Chem. Eng. Prog.* **1953**, 49, 585-590.

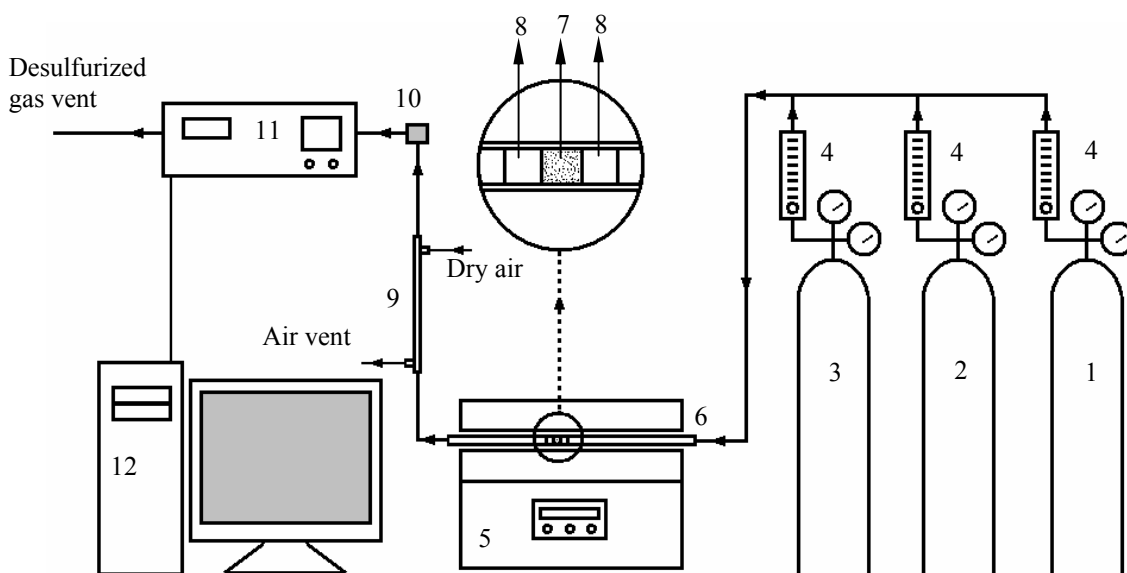


FIGURE 1. Experimental setup of the oxidation of SO<sub>2</sub>

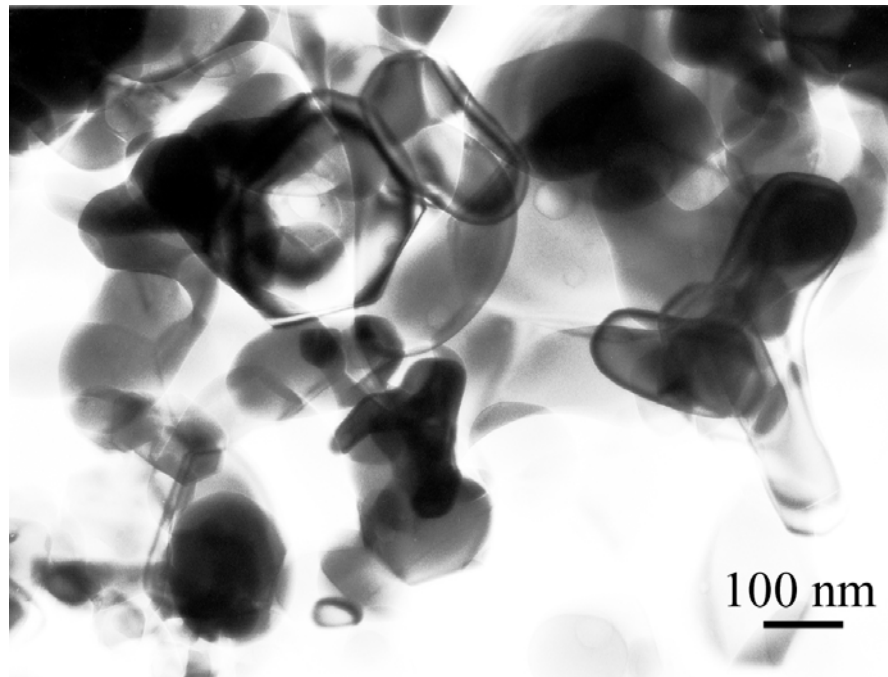
(1. Certified SO<sub>2</sub>; 2. Oxygen gas; 3. Nitrogen gas; 4. Flowmeter; 5. Lindberg/Blue M

TF55030A-1 tube furnace; 6. Quartz tube reactor; 7. Catalyst powder; 8. Quartz wool; 9.

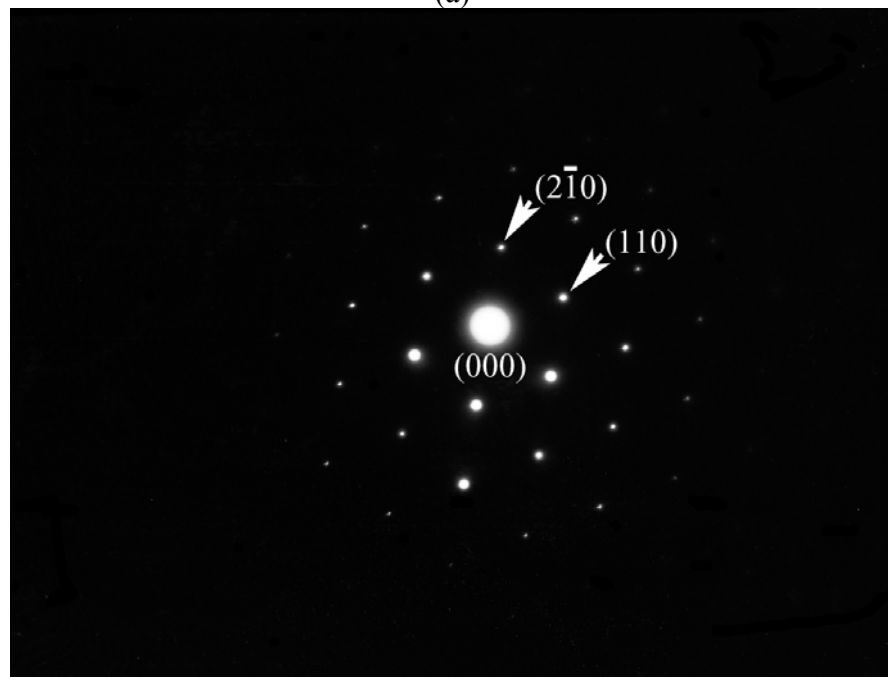
Permapure MD-110-48F-2 Nafion concentric tube dryer; 10. Particulate filter; 11. California

Analytical ZRF NDIR SO<sub>2</sub> analyzer; 12. Data acquisition system)



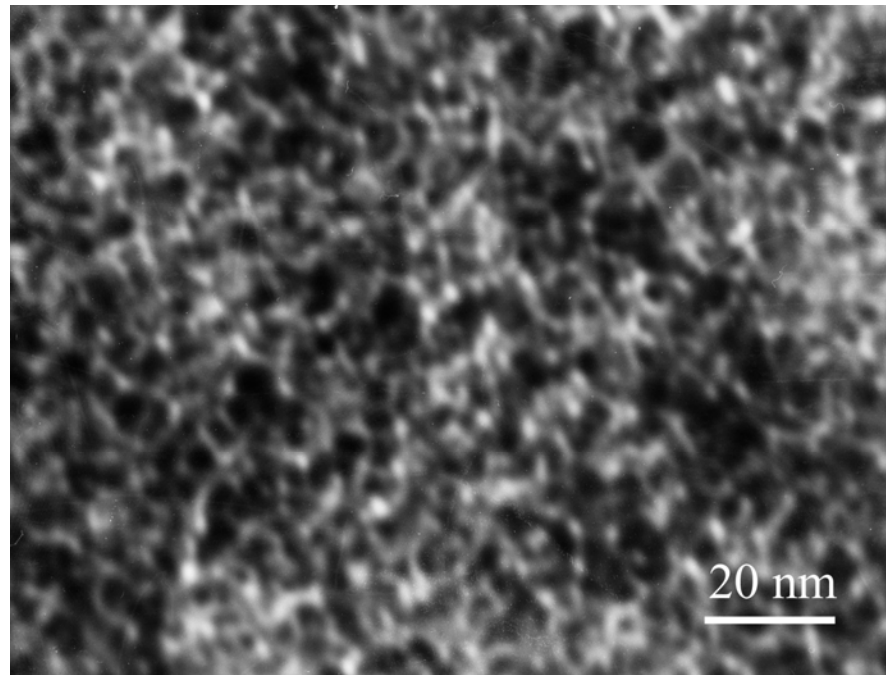


(a)

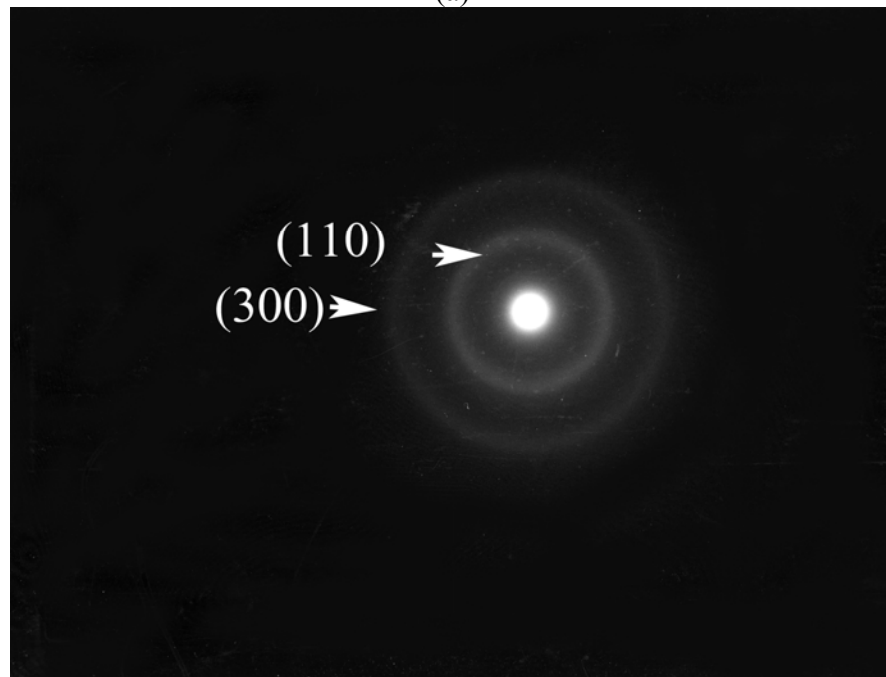


(b)

FIGURE 2. (a) Bright-field TEM image of the microscale  $\text{Fe}_2\text{O}_3$  particles; (b) selected area electron diffraction pattern of one of the microscale  $\text{Fe}_2\text{O}_3$  particle along the [001] zone axis.



(a)



(b)

FIGURE 3. (a) Bright-field TEM image of the nanoscale  $\text{Fe}_2\text{O}_3$  particles; (b) selected area electron diffraction pattern of the nanoscale  $\text{Fe}_2\text{O}_3$  particles.

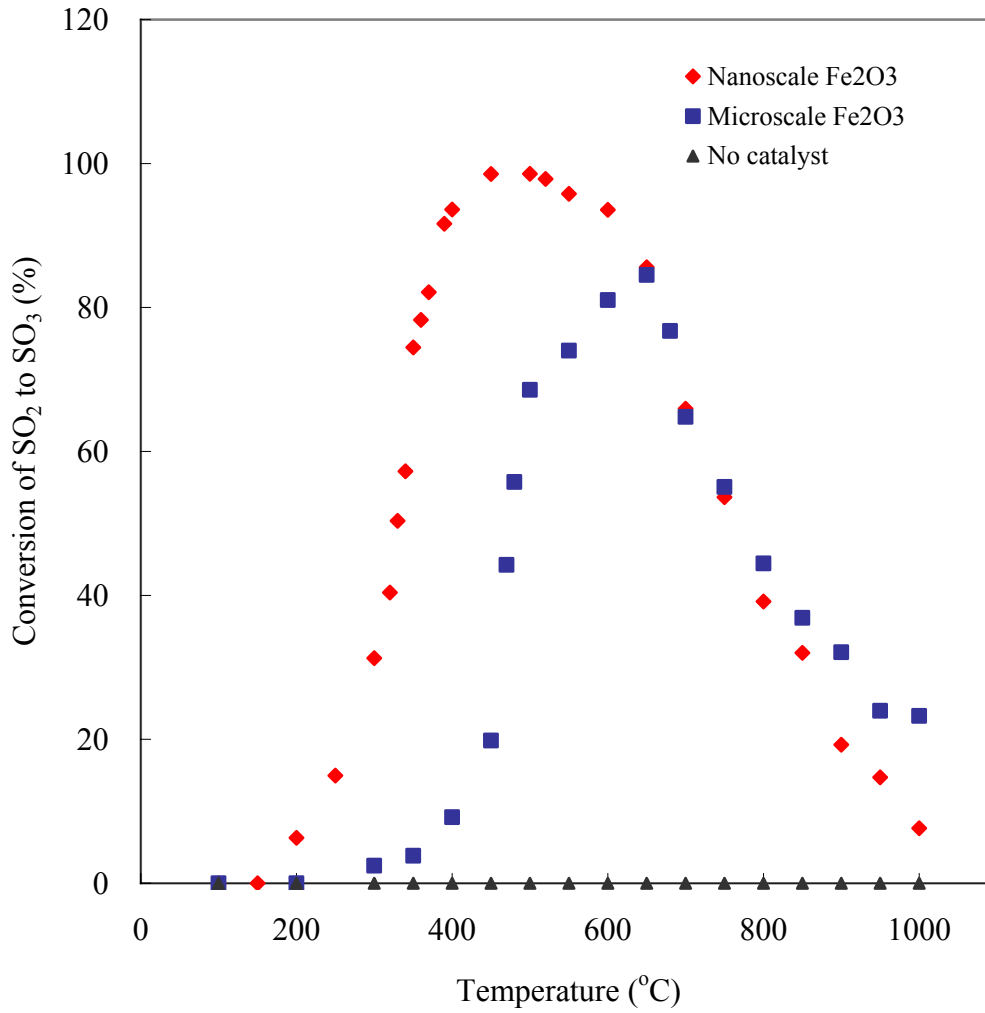


FIGURE 4. The effect of temperature on the conversion of SO<sub>2</sub> with respect to microscale and nanoscale Fe<sub>2</sub>O<sub>3</sub> (total flow rate: 50 mL/min; SO<sub>2</sub> concentration: 2000 ppm).

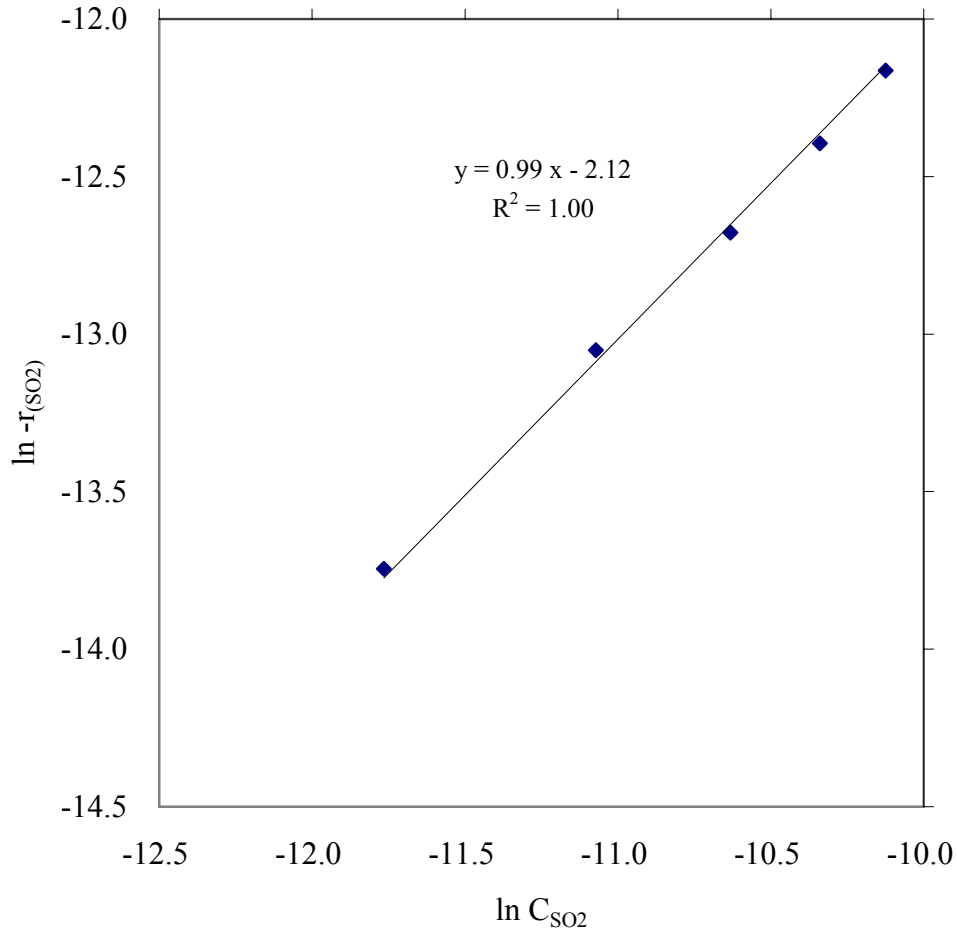


FIGURE 5. Determination of the reaction order for  $SO_2$ ,  $\alpha_{SO_2, Micro}$ , when microscale  $Fe_2O_3$  was used as catalyst (temperature: 500 °C; total flow rate: 50 mL/min; oxygen concentration: 50 v%;  $SO_2$  concentrations: 400, 800, 1200, 1600 and 2000 ppm).

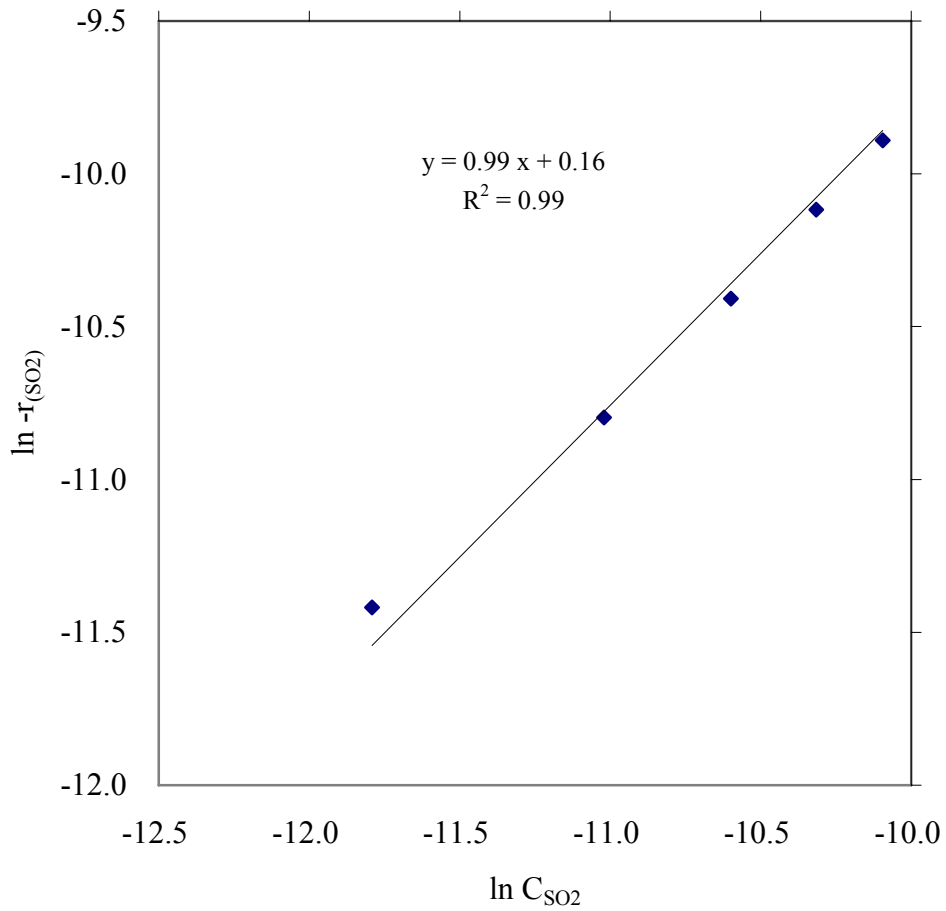


FIGURE 6. Determination of the reaction order for  $SO_2$ ,  $\alpha_{SO_2, Nano}$ , when nanoscale  $Fe_2O_3$  was used as catalyst (temperature: 320 °C; total flow rate: 50 mL/min; oxygen concentration: 50 v%;  $SO_2$  concentrations: 400, 800, 1200, 1600 and 2000 ppm)

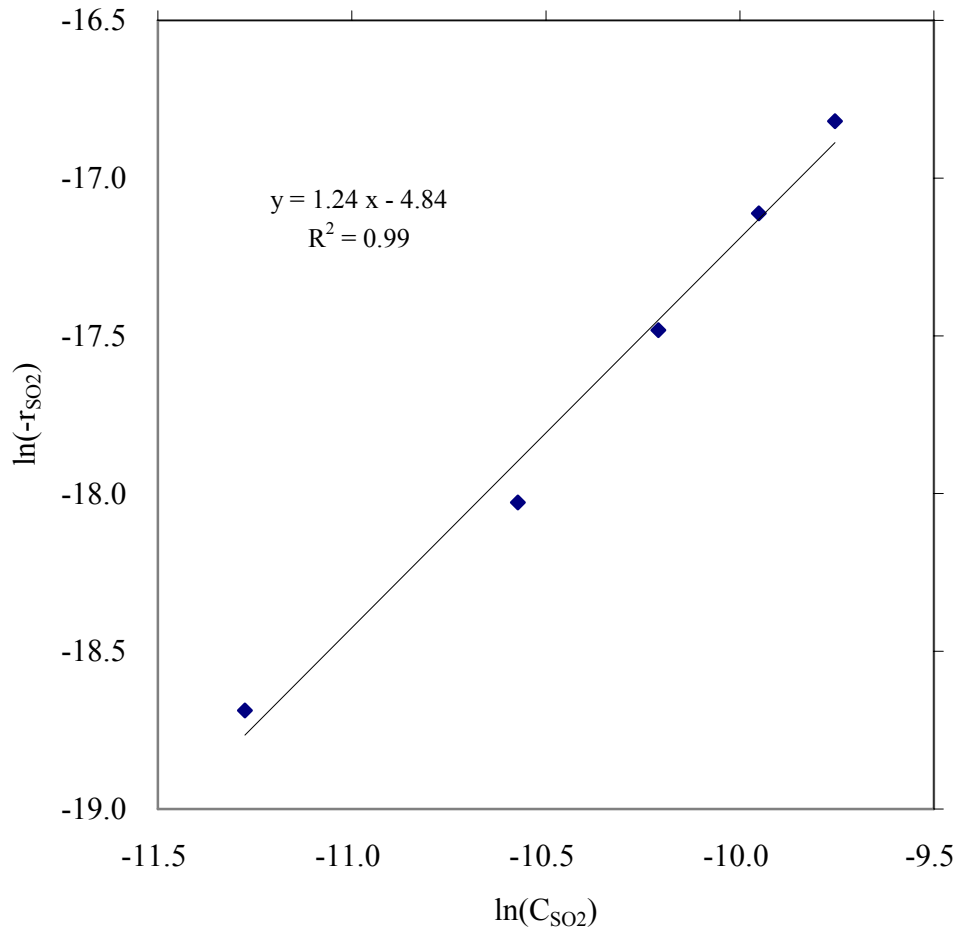


FIGURE 7. Determination of the reaction order for  $O_2$ ,  $\alpha_{O_2, Micro}$ , when microscale  $Fe_2O_3$  was used as catalyst (temperature: 650 °C; total flow rate: 50 mL/min; oxygen concentrations: 200, 400, 600, 800 and 1000 ppm;  $SO_2$  concentrations: 400, 800, 1200, 1600 and 2000 ppm).

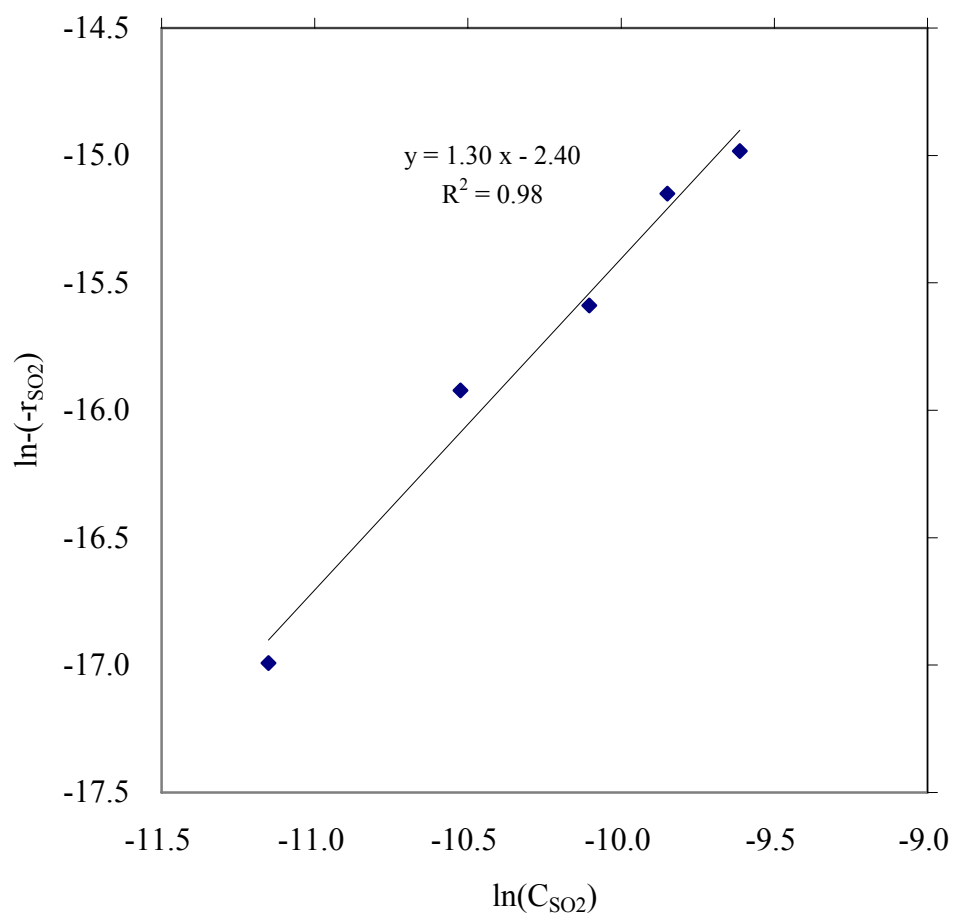


FIGURE 8. Determination of the reaction order for  $O_2$ ,  $\alpha_{O_2, Nano}$ , when nanoscale  $Fe_2O_3$  was used as catalyst (temperature: 400 °C; total flow rate: 50 mL/min; oxygen concentrations: 200, 400, 600, 800 and 1000 ppm;  $SO_2$  concentrations: 400, 800, 1200, 1600 and 2000 ppm)

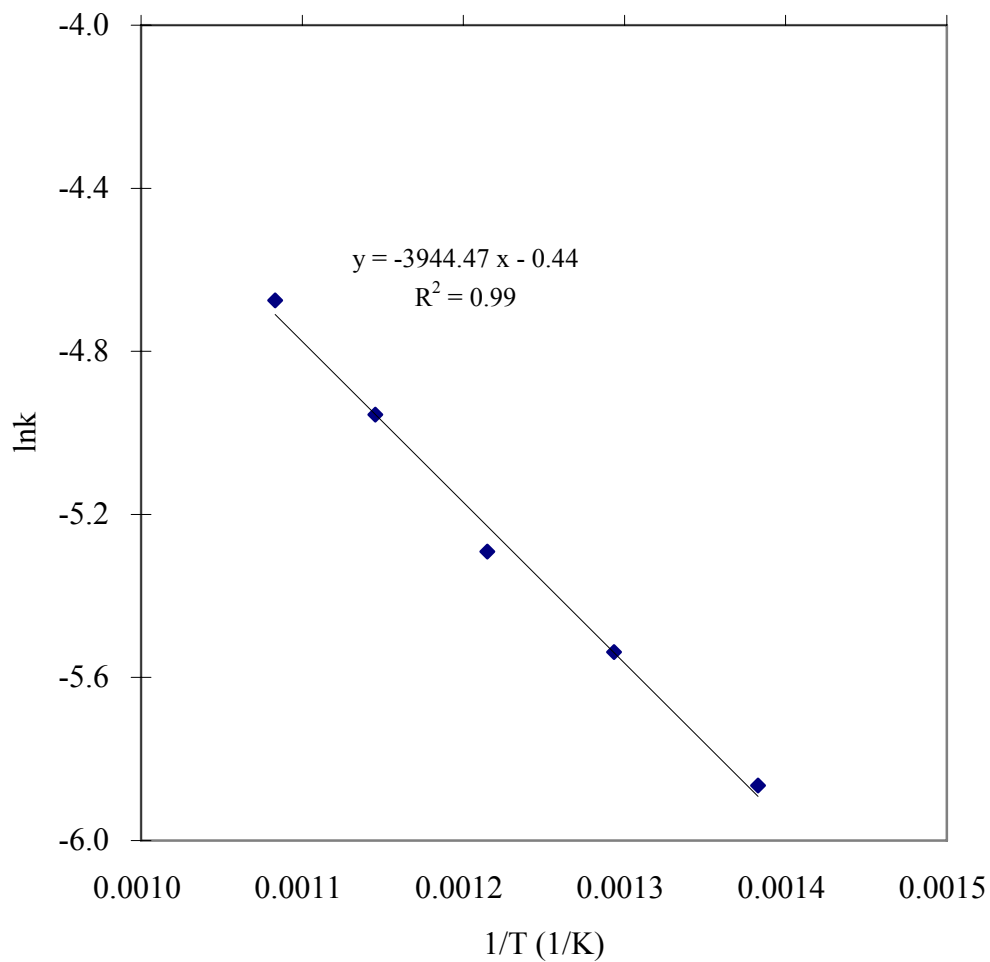


FIGURE 9. Determination of the apparent activation energy  $E_a$  and pre-exponential factor  $A$  for microscale  $\text{Fe}_2\text{O}_3$  catalyst (temperature range: 450 ~ 650 °C; temperature interval: 50 °C; total flow rate: 50 mL/min; oxygen concentration: 800 ppm;  $\text{SO}_2$  concentration: 1600 ppm).



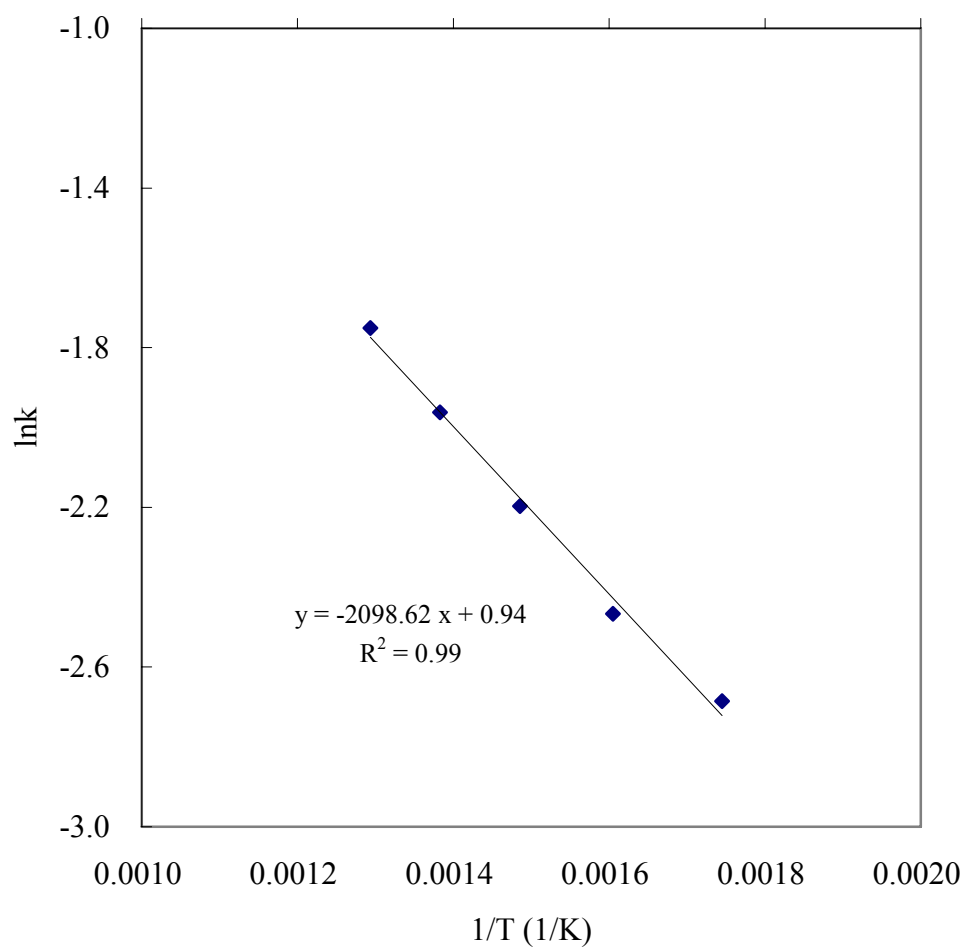


FIGURE 10. Determination of the apparent activation energy  $E_a$  and pre-exponential factor  $A$  for nanoscale  $\text{Fe}_2\text{O}_3$  catalyst (temperature range: 300 ~ 500 °C; temperature interval: 50 °C; total flow rate: 50 mL/min; oxygen concentration: 800 ppm;  $\text{SO}_2$  concentration: 1600 ppm).

TABLE 1. The physical properties and major chemical compositions of microscale and nanoscale Fe<sub>2</sub>O<sub>3</sub>

	Average particle size (nm)	Bulk density (g/cm <sup>3</sup> )	Fe <sup>2+</sup> concentration (wt%)	Total iron concentration (wt%)
microscale Fe <sub>2</sub> O <sub>3</sub>	100~200	0.5	0	69.5
nanoscale Fe <sub>2</sub> O <sub>3</sub>	3	0.05	0	69.4

TABLE 2. The reaction rate constant,  $k_{Micro}$ , at different temperatures for the reaction catalyzed by microscale  $Fe_2O_3$

Temperature (°C)	450	500	550	600	650
$k_{Micro}$ ( $mol^{-0.24} \cdot dm^{3.72} \cdot s^{-1} \cdot g^{-1}$ )	0.00284	0.00394	0.00504	0.00705	0.00933

TABLE 3. The reaction rate constant,  $k_{Nano}$ , at different temperatures for the reaction catalyzed by nanoscale  $Fe_2O_3$

Temperature (°C)	300	350	400	450	500
$k_{Nano}$ ( $mol^{-0.30} \cdot dm^{3.90} \cdot s^{-1} \cdot g^{-1}$ )	0.0682	0.0849	0.1112	0.1406	0.1736

## CHAPTER 5. GENERAL CONCLUSIONS

### Acetic Acid and Lactic Acid Recovery

Sulfur dioxide was proved to be an efficient alternative to strong acid to recover acetic acid and lactic acid from the calcium acetate and calcium lactate solutions. Organic acids were produced along with the calcium sulfite precipitate with the introduction of SO<sub>2</sub> gas into organic calcium salt solutions. The produced solid-liquid mixtures were treated with a simple filtration process to obtain free organic acids.

#### *Acetic Acid Recovery*

The experiment results showed that the time required for a complete reaction decreased with an increase of reaction temperature and SO<sub>2</sub> flow rate. The reaction time was found impropotional to SO<sub>2</sub> flow rate, which indicated that the reaction was complex and SO<sub>2</sub> flow rate was not the only controlling factor. Although a change of reaction conditions leads to a change of reaction time, analysis of the produced acetic acid concentrations demonstrated that the complete conversion of calcium acetate to acetic acid was not affected. The conditions of lower SO<sub>2</sub> flow rate and higher reaction temperature were found favorable to make use of SO<sub>2</sub> more efficiently at the expense of longer reaction time by comparing the yield of the reaction under different conditions.

#### *Lactic Acid Recovery*

The experiment results showed that both the reaction time and breakthrough time decreased with the increase of reaction temperature and SO<sub>2</sub> concentration, respectively. Analysis on the produced lactic acid concentrations indicated that the complete conversion of calcium lactate to lactic acid was not affected by the reaction temperature and SO<sub>2</sub> flow rate.

#### *Practical Application*

The recovery process can be designed using a higher SO<sub>2</sub> flow rate at room temperature without affecting recovery efficiency. Since energy for heating is substantially reduced, the latter feature is economically attractive for the industrial recovery of acetic acid and lactic acid from biological fermentation broth. Industry can either increase the flow rate of SO<sub>2</sub> containing gas or even use pure SO<sub>2</sub> gas. The findings of this study indicate that recovering acetic acid and lactic acid with SO<sub>2</sub> is both economical and environmentally beneficial.

### **Oxidation of SO<sub>2</sub> with Fe<sub>2</sub>O<sub>3</sub> as Catalyst**

#### *Catalytic Performance Evaluation*

The oxidation of SO<sub>2</sub> was greatly enhanced with the existence of either microscale or nanoscale Fe<sub>2</sub>O<sub>3</sub> according to the experiment results. Nanoscale Fe<sub>2</sub>O<sub>3</sub> performed much better than its microscale counterpart in catalyzing the SO<sub>2</sub> oxidation. It not only decreased the onset reaction temperature of SO<sub>2</sub> oxidation, but also improved the conversion of SO<sub>2</sub>. The conversion of SO<sub>2</sub> was temperature dependent for both types of Fe<sub>2</sub>O<sub>3</sub>. It increased with the temperature increase until it reached a maximum value, which is 84 % for microscale Fe<sub>2</sub>O<sub>3</sub> and almost 100 % for nanoscale Fe<sub>2</sub>O<sub>3</sub> respectively. The catalytic activity of Fe<sub>2</sub>O<sub>3</sub> was lowered after the optimum temperature, and the conversion of SO<sub>2</sub> decreased with the increase of temperature.

#### *Kinetics Model*

The kinetic models were established for SO<sub>2</sub> oxidation reactions catalyzed by both microscale and nanoscale Fe<sub>2</sub>O<sub>3</sub>. It was found that reaction of SO<sub>2</sub> oxidation were first order with respect to SO<sub>2</sub> for both types of Fe<sub>2</sub>O<sub>3</sub>. The reaction orders for O<sub>2</sub>, however, were different depending on the catalyst type. They were determined to be 0.24 and 0.30 for microscale and nanoscale Fe<sub>2</sub>O<sub>3</sub> respectively. The apparent activation energy of the reaction

catalyzed by nanoscale  $\text{Fe}_2\text{O}_3$  was 17.4 kJ/mol, which was only half of that for the reaction catalyzed by microscale  $\text{Fe}_2\text{O}_3$ . This fact explained the liability of the reaction taking place at lower temperatures with the use of nanoscale  $\text{Fe}_2\text{O}_3$  as catalyst. The experiment results demonstrated that nanoscale  $\text{Fe}_2\text{O}_3$  performed efficiently in facilitating  $\text{SO}_2$  oxidation. Considering its advantages of cost-effectiveness and environmental friendliness, nanoscale  $\text{Fe}_2\text{O}_3$  is expected to be a promising catalyst used for  $\text{SO}_2$  treatment.

**APPENDIX**





Figure 1. Experiment setup of organic acids recovery with  $\text{SO}_2$  (1.  $\text{SO}_2$  source; 2.  $\text{N}_2$  source; 3.  $\text{SO}_2$  and  $\text{N}_2$  mixture inlet; 4. 500 mL Reaction vessel; 5. Neslab RTE-111 bath/circulator; 6. Condenser; 7. Outlet gas drying system; 8.  $\text{SO}_2$  flowrate controller; 9.  $\text{N}_2$  flowrate controller)



Figure 2. Experiment setup of the oxidation of  $\text{SO}_2$  with  $\text{Fe}_2\text{O}_3$  as catalyst (1. Nitrogen gas; 2. Certified  $\text{SO}_2$ ; 3. Oxygen gas; 4. Flowmeter; 5. Quartz tube reactor; 6. Lindberg/Blue M TF55030A-1 tube furnace; 7. Permapure MD-110-48F-2 Nafion concentric tube dryer; 8. California Analytical ZRF NDIR  $\text{SO}_2$  analyzer; 9. Data acquisition system)



Figure 3. The microscale iron oxide sample



Figure 4. The nanoscale iron oxide sample

**ACKNOWLEDGEMENT**

These studies were carried out under the direction of the author's ex-advisor, Dr. Maohong Fan. The author appreciates his valuable suggestion and great help on the research design and data analysis. In addition, the author expresses gratitude for the assistance of Soon-Chul Kwon in Department of Civil, Construction, and Environmental Engineering at Iowa State University.